LSU Master's Theses   Graduate School

2007

A liquid lens based on electrowetting

Jihwan Park

Louisiana State University and Agricultural and Mechanical College, jpark12@lsu.edu

Recommended Citation

A LIQUID LENS BASED ON ELECTROWETTING

A Thesis

Submitted to the Graduate Faculty of the
Louisiana State University and
Agricultural and Mechanical College
in partial fulfillment of the
requirements for the degree of
Master of Science in Electrical Engineering

in

The Department of Electrical and Computer Engineering

by
Jihwan Park
B.S., Korea Military Academy, 1997
August 2007

TABLE OF CONTENTS

LIST OF TABLES

LIST OF FIGURES

ABSTRACT

A primary goal of this work is to develop and characterize a novel liquid lens based on electrowetting. A droplet of silicone oil confined in an aqueous solution works as a lens. Electrowetting then controls the shape of the confined silicone oil, and the focal length may be varied upon an applied electric potential. The planar lens design is employed for easy integration of a lens system into a microfluidic device. The achievements of this work are to develop an electrowetting-based planar liquid lens without an off-the-plane electrode structure and to demonstrate the planar liquid lens with variable focal length control.

Electrowetting has recently become popular in many applications including a liquid lens. However, reported liquid lenses based on electrowetting had a limitation of integration onto a lab-on-a-chip system due to their off-the-plane electrode structures. In order to overcome the structural issue, a planar liquid lens is proposed in this thesis. A silicone oil droplet confined in an aqueous solution acts as a lens material. Planar ring-type electrodes control the confinement of silicone oil by electrowetting. With an applied potential, the surface above the ring-type electrodes becomes hydrophilic and attracts the surrounding aqueous solution making the confined silicone oil more curved. By charging the curvature of the lens, the focal length can be controllable.

As the lens is in a planar shape, it will be simple to integrate the planar lens on a microfluidic system. The lack of a vertical wall requirement in the demonstrated liquid lens eliminates the limitation of the integration issue for lab-on-a-chip systems. In addition, due to the controllable variable focal length of this lens, it is applicable to various optical applications which need an integrated and controllable lens.

CHAPTER 1. INTRODUCTION

1.1 Overview

This thesis presents the development and demonstration of a liquid lens based on electrowetting. Essentially, variable focal length liquid microlenses are being used to create the next generation lenses for a wide variety of microelectromechanical systems (MEMS) applications. In real-time operation, the application of a voltage causes the lens to change its focal length. The liquid lens recovers its initial focal length upon removal of the voltage.

Taking a wettability mechanism approach, surface properties are determined by contact angles of different test liquids on the samples due to their unique surface energies. Based on the Lewis theory of acids and bases [1], the wettability of different surfaces is derived using the Zisman method [2].

To investigate actuation mechanism, electrowetting is incorporated into the design of a liquid lens. This electrowetting mechanism is considered to be a potential surface modification process to change between hydrophobic and hydrophilic surfaces using applied electric potential. The actuation mechanism study includes not only electrowetting as the surface modification method, but also wettability of different surfaces.

Based on this electrowetting, a planar liquid lens design, consisting of two immiscible liquids such as oil and water, is developed. Non-polar oil as a lens is immersed in water as an actuating liquid and should be confined to the center position. Ring-shaped electrodes, covered by a hydrophobic layer, are employed to confine oil inside the water and to actuate the confined oil by electrowetting. By applying electric potential on the electrodes, the shape of the oil droplet that forms the lens is changed. The focal length of the lens also varies, according to different oil droplet dimensions.

To yield optical properties of the liquid lens, the focal length is characterized by using dimensions of the liquid droplet. The correlation between the focal length and the numerical aperture data is good for the variable focal length range considered. Finally, this study shows how the liquid lens design can be extended for applications in integrated microsystems.

1.2 Research Goals

The goals of this research are:

1) To analyze surface wettability based on surface energy with contact angle measurements;

2) To verify active surface modification based on electrowetting due to electric potential difference;

3) To examine the competitive electrowetting between electrolyte and oil, and

4) To design, fabricate, and characterize the liquid lens.

Reported liquid lenses are limited to the integration of lab-on-a-chip and off-the-plane structure [3-5]. Although it is useful to some extent, limited applications reflect the need for improvements. This current status of liquid lens research reflects the need for design flexibility, especially if a more complicated system is to be considered. An attempt to fill this void has motivated this thesis work on the electrowetting-based liquid lens.

1.3 Thesis Outline

The main body of this thesis comprises six chapters.

Chapter 2 discusses the background for research on a liquid lens based on electrowetting. An overview of various microlenses is given.

Chapter 3 describes the wettability of surfaces studied on the basis of surface energy and surface tension. Several different surface properties are arranged by specific theories.

Chapter 4 presents the electrowetting phenomenon which describes the behavior of electrolyte droplets on the dielectric layer. Also, the competitive electrowetting of oil-water phase is experimentally studied.

Chapter 5 presents the liquid lens, based on electrowetting that demonstrates the variable focal length of the lens. The design and fabrication of the liquid lens is described in detail. Experimental results of the liquid lens are also presented.

Chapter 6 summarizes the achieved work and suggests possible future research activities.

CHAPTER 2. BACKGROUND AND RESEARCH MOTIVATION

2.1 Introduction

2.1.1 A Brief History of Optical Lenses

The history of the lenses dates back to 2000 B.C., when the magnifying power of lenses was discovered by Klaudios Ptolemaeos in Greece [6]. The Greeks used polished quartz or beryl as a lens material. From the 14th century onward, glass played an important role as a lens material.

The light that passes through a lens defines the magnified image. The typical component of optical lenses is made of glass that produces images by refraction. The lens has a long history of using glass as the main material. Recently, polymers or novel materials have been used instead of glass, which exhibits heavy weight and fragile properties.

The optical lens plays a leading role as an instrument used in man's efforts to magnify objects. In addition to the examination of historical records, a study of basic optics can be used to evaluate the optical performance of the lens.

2.1.2 Basic Optics

Visible light is electromagnetic radiation that travels straight in a vacuum, and hence it is impossible to converge without other materials [6]. However, the refractivity of light makes it possible to converge or diverge by using different media.

Every lens is characterized according to its focal length. Focal length is defined as the distance from the lens to the focal point along the optical axis. It is usually denoted by f. Figure 2.1 illustrates the focal length of a lens. Diopter, or lens power, is defined as the reciprocal of a focal length. The focal length is regarded as a critical factor of lens performance.
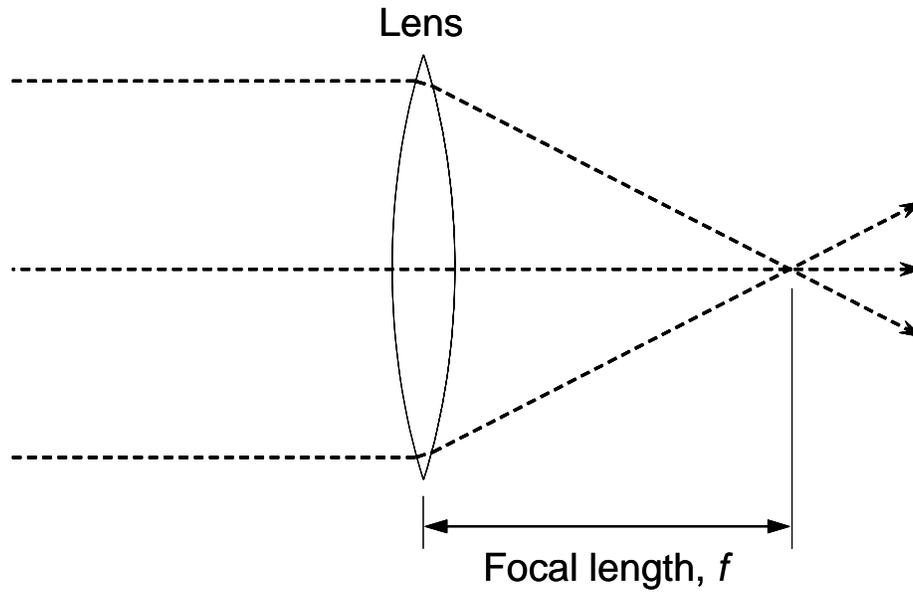
Figure 2.1. Schematic illustration of a focal length.

Willebrord Snel van Royen (1591-1626), a French mathematician, observed the laws of refraction. He correctly concluded the relationship between angles of incidence and refraction:

$$n_1 \sin \theta_1 = n_2 \sin \theta_2 \qquad\qquad (2.1)$$

where θ_1 and θ_2 refer to incident angle and refracted angle, respectively.
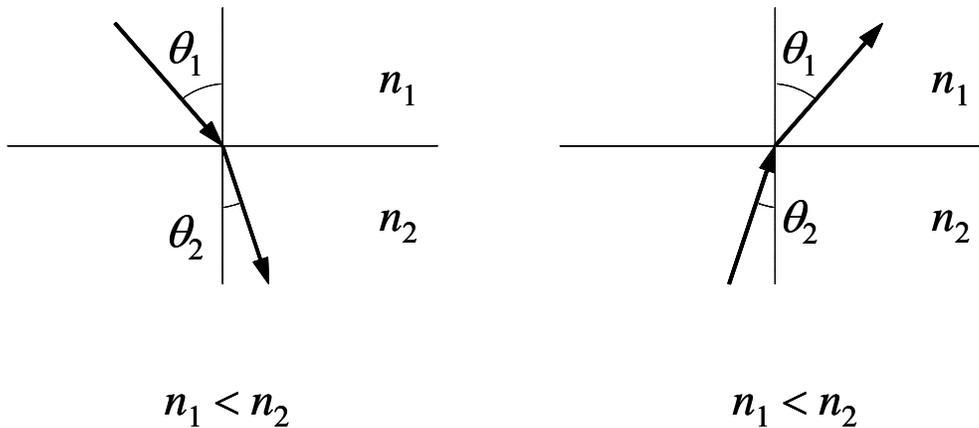
Figure 2.2. Refraction of light at the interface of two different media.

The refractive index of two different media is described by n_1 and n_2. Small refractive index can be expressed by a fast medium, and large refractive index can be expressed by a slow

5

medium. If light passes from a fast medium to a slow medium, then the incident light is refracted toward the vertical axis of a slow medium and vice versa, as illustrated in Figure 2.2.

2.2 Lens in Microsystems

2.2.1 Microlens

Microelectromechanical systems (MEMS) that respond to electric and mechanical devices have been developed from the 1980s. Recently, numerous microscale components were developed in the MEMS area, and a microlens is one of those components. Literature reported various aspects of microlens applications. A microlens may be defined as a tiny-sized lens which has a diameter in the order of several hundreds or thousands of micrometers or less. A microlens can be either a single aperture lens or a microlens array [7].

A lens in microsystems provides the function of imaging or optical guiding [7]. In imaging applications, microlenses can intensify optical signals. An example is the detection of fluorescent light in μ-TAS (Micro Total Analysis System) [8-9]. On the other hand, microlenses facilitate the function of light beam splitting [10] or optical switching [11-12] in optical guide applications. Generally, a microlens can be divided into two major categories based on its focal length: a fixed focal length microlens and a variable focal length microlens.

2.2.2 Fixed Focal Length Microlens

Various fixed focal length microlenses [8-9] and microlens arrays [13-15] have been reported for optical applications in microsystems. Typically, microlens arrays are made by photoresist or polymer. The lens shape may be achieved by reflow of photoresist or polymer after photolithography [16]. Often a hot embossing technique is also employed to form a microlens array on a polymer substrate [17]. Fixed focal length microlens arrays have been used for optical signal guidance in optical communication systems [13]. A fixed focal length microlens has a simple structure and is easy to fabricate at low cost, but its applications are limited if an active optical control is necessary.

2.2.3 Variable Focal Length Microlens

Most macroscale optical systems mechanically displace lenses to control the focal length of the system. When mechanical parts are reduced in size for a miniaturized optical system, the surface-to-volume ratio is increased, and thus the friction problem is increased significantly. For example, when the length of mechanical parts is reduced by 10 times, the friction is increased by 10 times [18]. It may influence the overall performance of microdevices. Conventional control of a focal length in a microscale will be accompanied by problems such as complicated fabrication and assembling processes applying tiny components, large power consumption, and huge friction. A variable focal length lens in microsystems must address those problems for reliable operations.

The human eye is one of the good examples of variable focal length lenses. The crystalline lens is deformed by ciliary muscle [19]. Mimicking the human eye, several variable focal length microlenses have been reported in the past years. They employed by simple actuation methods including pneumatic actuation [20-21], thermal actuation [22] and electrostatic actuation [3, 23]. The following section describes three different kinds of variable focal length microlenses: polymer-based lens, liquid crystal lens, and liquid lens.

2.3 Literature Review of Variable Focal Length Microlenses

2.3.1 Polymer-Based Variable Focal Length Microlens

In recent years, research in polymers has matured rapidly, finding better methods to fabricate microstructures. Polydimethylsiloxane (PDMS) has become a popular material in microscale applications because it is transparent, chemically inert, and mechanically flexible. Due to its transparent property, PDMS has been used to fabricate a polymer-based microlens [24].

Figure 2.3 shows the structure of a polymer microlens actuated by a pneumatic pressure. Thin PDMS layers are bonded on a glass substrate, forming a chamber [25-26]. The actuating liquid, usually water that has high transparency, is filled inside the PDMS chamber and is connected with a microfluidic system and a pneumatic pump [26]. The PDMS layer changes its shape when liquid flows in and out of the chamber [21] and the focal length of the lens is varied by the pneumatic pressure [26]. In recent work, Varahramyan *et al.* reported the focal length variation of $\pm 3.1 \sim \pm 75.9$ mm [20].
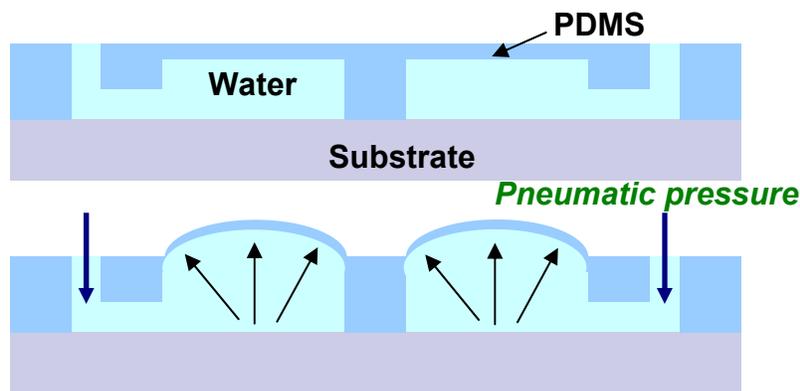
Figure 2.3. Schematic diagram of the polymer microlens by pneumatic actuation [20-21].

On the other hand, one of the greatest drawbacks of the polymer-based microlens is the pneumatic pump involved. Also, porous PDMS membrane [24] will degrade optical quality of the lens.

Ionic electroactive polymers are one of the possible materials for a polymer-based variable focal length microlens. Paxton *et al.* reported that swelling hydrogel in a sodium chloride (NaCl) solution could be used as a lens material [27]. The hydrogel swelling is achieved by applied electric fields [28]. However, there are many challenges to overcome before the realization of a microlens using this new approach.

2.3.2 Liquid Crystal Lens

Liquid crystal refers to the intermediate state between liquid state and solid state as invented in 1976 by W. J. Jackson in the Eastman Kodak company [29]. The liquid crystal is divided into two categories: nematic liquid crystal and smectic liquid crystal. Usually, the nematic liquid crystal is recognized as a typical liquid crystal. The liquid crystal consists of two components which include several flexible part molecules and mesogens, as rod-shaped, solid, part molecules [30]. The mesogens in the smectic liquid crystal are more oriented than the mesogens in the nematic liquid crystal; therefore, the nematic crystal presents optical properties as good as those of an optical filter [29]. As a result, a rod-shaped, cross-linked polymer, such as mesogen in liquid crystals, offers electric field-induced optical alignment [28].

Since early 1980s, numerous research interests were directed toward the development and characterization of liquid crystals. As mentioned earlier, their most attractive feature is the ability to control the orientation of alignment with an applied electric field. The most useful applications are liquid crystal display, optical beam steering [31], and liquid crystal microlens [23].

Studies of a variable focal length liquid crystal microlens that exhibited focal length change when subjected to electric field were reported in the 1970s [32]. Sato reported that an electric field induces a change in the refractive index of a lens made by using the nematic liquid crystal [32]. Commander *et al*. demonstrated a liquid crystal lens by using both diverging lens and converging lens [23]. In these applications, birefringence may be considered the fundamental principle of focal length change in a liquid crystal lens. The liquid crystal lens is formed by sandwiching a nematic liquid crystal layer between two transparent indium tin oxide (ITO) electrodes. If the voltage is applied to the electrodes, the direction of a solid-like mesogen

aligns itself in parallel or perpendicular to the optical axis. Figure 2.4 shows that the different

orientation of mesogens in a nematic liquid crystal could be utilized of as a lens [32].
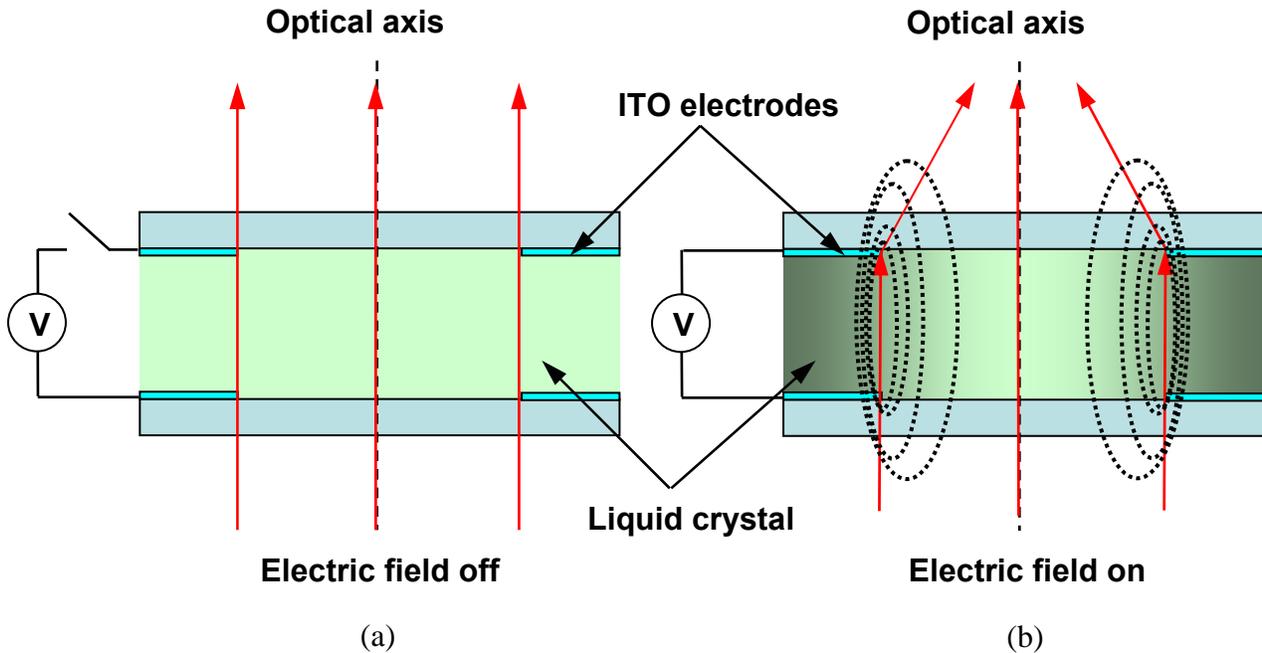
Figure 2.4. Concept of a liquid crystal lens: (a) the refractive index of liquid crystal is uniform when the electric field is off and (b) the refractive index of liquid crystal near the electrodes is different from the center area when the electric field is on.

When no electric field is applied, the refractive index of liquid crystal is uniform and the

liquid crystal works as a simple filter. On the other hand, when the electric field is applied on

the electrodes, the refractive index of liquid crystal near the electrodes is changed and hence the

liquid crystal becomes a lens [32]. According to Commander *et al.*, the focal length transition

occurs in the range of 2 V to 12 V, exhibiting focal length changes that can reach 490 μm to

1000 μm with a liquid crystal lens [23]. It is also reported that a liquid crystal lens can attain

focal length changes with low applied voltage [33]. However, a liquid crystal lens often

showed disclination lines caused by the non-uniform property of liquid crystals [34].

2.3.3 Liquid Lens

A liquid droplet forms a curved surface, and hence can be used as a lens [35]. The shape of a liquid droplet on a solid surface can be controlled by surface tension or by a surface modification such as wetting. Surface tension is dramatically large in a very small volume of water, in the range of 10~100 μl [5]. Electrowetting is known as a technology that controls the surface tension in liquid droplet using an electric potential and has been applied to various liquid droplet control systems in microscale [36]. Using electrowetting, there have been several reports on microscale liquid lens applications by Krupenkin *et al.* [5], Berge *et al.* [37], and Hendriks *et al.* [3] as shown in Figure 2.5.

The design in Figure 2.5 (a) consisted of a conducting liquid that acted as a lens surrounded by air. The applied electric potential altered the surface wettability, and thus the liquid droplet changed its shape. The device showed the concept of a liquid droplet lens, but it also revealed a few problems. The liquid droplet alignment was not easy to obtain. Also, the droplet could easily evaporate without a humidity chamber, and hence could not be applicable for a practical use.

Figure 2.5 (b) shows a liquid lens with a geometrical cavity shape structure [37]. In this design, an oil droplet acts as a lens surrounded by conductive water instead of air, which eliminates the evaporation problem. The interfacial tension between water and oil is controlled by electrodes on the geometrical bowl. However, it requires cavity structures of a 3-dimensional circular shape, and hence it has several limitations in using current microfabrication processes.

In 2004, Hendriks *et al.* (at Philips in the Netherlands) demonstrated a liquid lens with a vertical electrode structure, as shown in Figure 2.5 (c) [3]. This liquid lens consists of immiscible oil and water, where the water droplet has a spherical lens shape without any applied electric voltage. When an electric voltage is applied, water comes along the vertical electrodes, oil curvature is changed to a spherical shape, and its focal length is changed.
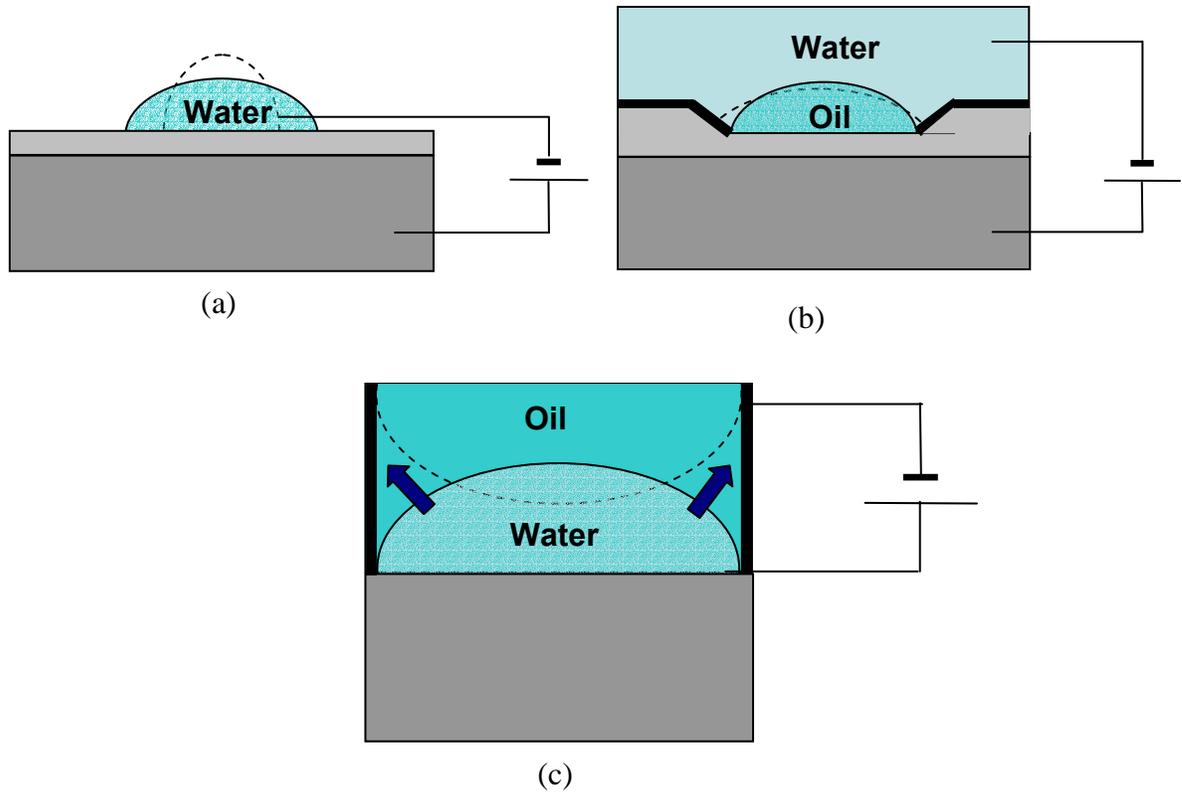
Figure 2.5. The schematic diagram of different liquid lenses: (a) the conducting liquid itself which acts as a lens [5]; (b) the liquid lens with a geometrical cavity [37], and (c) the two immiscible liquids which glass wall [3].

The advantages of liquid lenses are fast response time, low power consumption, and reversibility without any mechanical parts [3-4]. However, the liquid lenses have fundamental problems such as liquid evaporation, a high electric field for the actuation mechanism, and a size limitation [3-5, 37]. A liquid lens with a diameter greater than 5 mm is prone to severe optical distortion due to a gravity effect and it has an aberration problem caused by a non-uniform lens shape [3]. Finally, all reported liquid lenses are difficult to integrate into lab-on-a-chip systems, due to bulky and complicated structures.

2.4 Problem Statement and Present Approach

2.4.1 Problem Statement

This chapter studied the literature review of microlenses. Microlenses are divided by two categories, a fixed focal length microlens and a variable focal length microlens. In microscale, conventional control of a focal length based on the mechanical actuation of a fixed focal length lens has problems such as huge friction and large power consumption. Therefore a variable focal length lens is desired in microsystems.

A liquid lens has recently become an attractive alternative to a variable focal length microlens due to its fast response time, low power consumption and reversibility [3-4]. However, despite the recent demonstration of liquid lenses, a major problem that exists with microsystems is the off-the-plane design [3, 37].

A vertical electrode or a geometrical cavity is considered to be an essential component in the previous liquid lenses [3, 37]. However, the off-the-plane structure could affect design flexibility and it had a limitation to integrate microsystems. In addition, the off-the-plane electrodes require complicated fabrication.

2.4.2 Present Approach

The main motivation of this thesis work is to develop and demonstrate a liquid lens based on electrowetting. As mentioned in the previous section, the off-the-plane electrode structures of liquid lenses have limitations in integration. A new planar lens design does not have off-the-plane electrodes and, therefore, it is applicable to integrate onto microfluidic systems. In this work, planar ring-type electrodes are employed in order to control liquid droplet shapes using electrowetting.

The trade-off in using a planar lens design is a challenge in confining a liquid droplet. The oil droplet surrounded by water acts as a lens and is placed on a polymer surface. Since the

water in which the oil is immersed is unstable on a polymer surface, it tends to get dispersed and mobile. This problem could be addressed by controlling the property of the polymer surface using electrowetting. Another electrode pattern that surrounds the confined oil droplet is added to control the surface property of the polymer substrate. This surrounding ring-type electrode helps to confine the oil droplet as it attracts water molecules around the oil droplet.

CHAPTER 3. WETTABILITY OF SOLID SURFACES

3.1 Introduction

In the morning, we can see water droplets on leaves and widows. Each water droplet has a distinct shape, due to the different surface properties possessed by leaves and windows. These surface properties are determined by the surface energy of the surface. While the surface energy is one way of characterizing a solid surface, surface tension is another way of characterizing liquid on a solid surface [2].

The molecules of liquid interact uniquely on different solid surfaces. These different interactions of liquid on each solid surface can be characterized by wetting [1]. Wettability is defined by different wetting phenomena, and it can be determined by a liquid droplet shape [1]. It can be seen that water droplets retain shape as the droplets drift along the surfaces of the leaves, yet water droplets tend to spread along the surfaces of window glass. This can be explained by the low wettability of the leaves and the high wettability of the window glass.

Every liquid droplet forms a different shape on various solid surfaces. The angle of the interface between a liquid droplet and a solid surface is called a contact angle. A contact angle can be used to determine wettability [38]. A low contact angle means high wettability, and a high contact angle means low wettability [1]. Wetting means that the contact angle between a liquid and solid is less than $90°$, while dewetting means that the contact angle is greater than $90°$ [1].

These surface properties of solids cannot be easily changed without chemical treatment. However, in the 1990s, an electrowetting concept was developed which allows surface modification by electric fields [36]. Electrowetting will be described in Chapter 4.

3.2 Contact Angle

3.2.1 Concept of Contact Angle

The shape of a water droplet on a solid surface depends on the surface property of the solid. Wettability is a unique aspect of liquid reactions on different solid surfaces [2]. The surface energy is measured using the Lewis theory of acids and bases [1]. Surface energy determines the wettability of a solid surface [1], and a contact angle of liquid varies with different solid surfaces. The contact angle measurement is one of the methods used to estimate surface energy.

In 1805, Thomas Young discovered that the contact angle describes the interfacial effects among solids, liquids, and vapors at the edge of a liquid droplet, far from the core region [1]. Figure 3.1 shows a schematic diagram of contact angle on the edge of a liquid droplet.
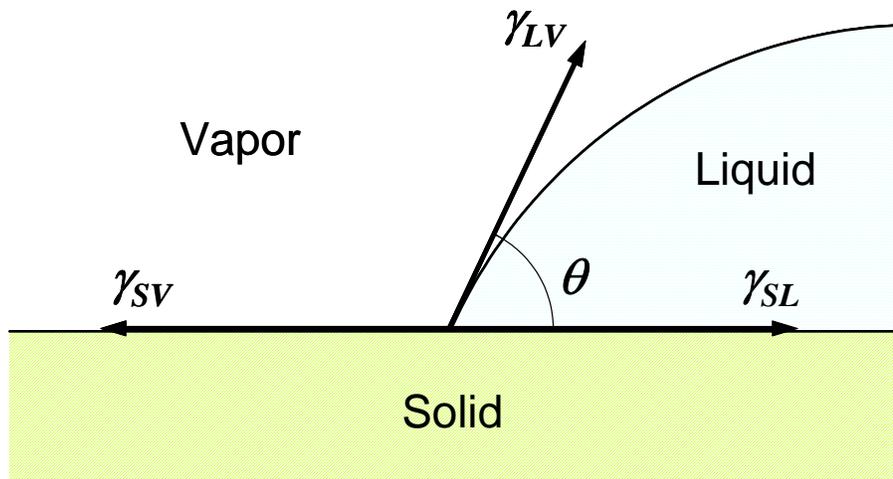
Figure 3.1. Schematic diagram of contact angle at the edge of a liquid droplet.

Each interface has a certain free energy per unit area and is expressed by γ_{SL}, γ_{SV} and γ_{LV}. These stand for free energy between a solid and a liquid, a solid and a vapor, and a liquid and a

16

vapor. The Young's equation that describes the relationship of free energy among the three phases is [2]:

$$\gamma_{SV} = \gamma_{SL} + \gamma_{LV} \cos\theta .$$ (3.1)

When the contact angle is equal to zero, it is called complete wetting. If the contact angle has a certain value, it is called partial wetting [38].

The contact angle is divided into two categories, which are the static contact angle and the dynamic contact angle. Usually a static contact angle is used for measuring wettability of surfaces, and a dynamic contact angle is used to measure the contact line in motion. A dynamic contact angle can be further classified into an advancing contact angle and a receding contact angle, depending on whether the solid and liquid interface area is increasing or decreasing, respectively [38].

3.2.2 Contact Angle Measurement

A static contact angle can be measured by a liquid droplet shape on solid surfaces. A contact angle goniometer is an effective method to measure a static contact angle. FTA 125 contact angle analyzer from First Ten Ångstrom (Portsmouth, Virginia) was used as a contact angle goniometer. It consists of three parts: a digital camera, an illuminator, and image processing software. The system has the capability to measure the surface tension and the contact angle and to calculate the surface energy and adhesion characteristics from the measured data. The contact angle goniometer is shown in Figure 3.2.

3.3 Surface Properties

3.3.1 Surface Energy and Surface Tension

Surface energy is the collective excess energy of unbounded molecules at the surface of materials [2]. In the bulk of a solid, the molecules are energetically stabilized, whereas the boundary area has unbounded molecules, which are subjected to excess energy. This excess

energy at the boundary area of a solid surface is called surface energy [1]. The unit of surface energy, or energy per unit area, is erg/cm^2 or J/m^2. However, its equivalent value, force per unit length, is called surface tension and the unit is dyne/cm or N/m.
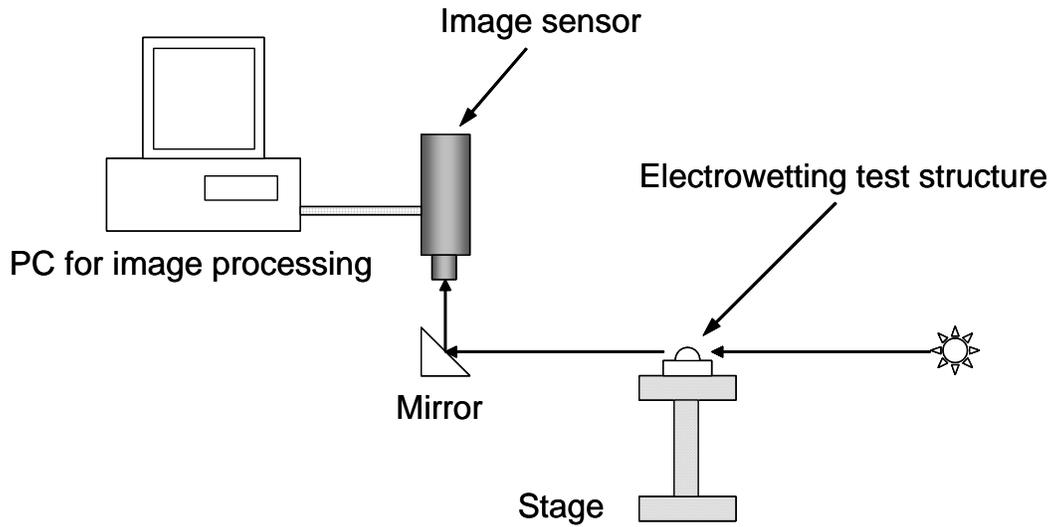
(a)

(b)

Figure 3.2. Contact angle measurement system: (a) schematic diagram and (b) a photograph of the system.

Surface property may be expressed by the surface energy as a scalar value, or the surface tension as a vector value, between the solid and liquid interface [1-2]. The surface energy cannot be measured directly, but the surface tension can be measured by a liquid droplet shape. Liquids have different contact angles, depending on the surface energy of the contacting solid materials. Contact angle measurement is a useful way to determine the surface energy.

There are several models to estimate the surface energy by using contact angle measurement. The Zisman plot has emerged as a powerful method for determining the surface energy [39]. Zisman has inferred that wettability is characterized by the work relationship between the adhesion force in the liquid-solid interface and the cohesion force in the liquid [1]. In (3.1), the work of adhesion (W_a) can be represented by the following equation [39]:

$$W_a = \gamma_{LV}(1 + \cos\theta). \tag{3.2}$$

This adhesive force acts on spreading liquid on the surface. In contrast, cohesive force (W_c) acts on shrinking liquid on the surface [39]:

$$W_c = 2\gamma_{LV}. \tag{3.3}$$

When this physical principle is exploited as a surface property measurement technique, the combined equation results in:

$$W_a = \frac{1}{2}(1 + W_c \cos\theta). \tag{3.4}$$

Zisman inferred that the competition of cohesive forces and adhesive forces results in a certain contact angle. These unique contact angles have different values on various liquids. Critical surface tension is described as a point with zero contact angle. The critical surface tension can be expressed by complete wetting. However, there are no existing liquids on solids that have critical surface tension property. Any liquid has a certain contact angle, which is greater than zero. This critical surface tension may be represented by surface energy. Each liquid has a

unique surface tension, γ_{LV}, and a contact angle for a given solid. The relationship between the contact angles and surface tensions of various liquids can be plotted using an extrapolation technique, thereby arriving at the critical surface tension (CST) of the solid surface.
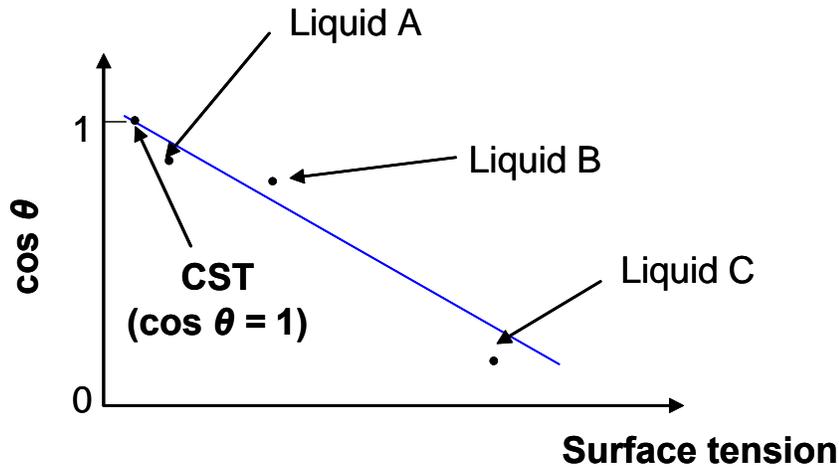
Figure 3.3. Zisman plot for determining surface energy [39].

Zisman's critical surface tension model commonly employs thermodynamic approaches that have been successfully applied to surface properties. The main problems with the technique come from a neglect of correlation effects of polar and dispersive components of molecules. The Zisman model may only be applied to low energy surfaces [1], but it causes no problem in this work. Although there are several methods for determining surface energies, the Zisman method is employed in this chapter because we can estimate the surface energy of a solid using the critical surface tension [39].

3.3.2 Hydrophilic and Hydrophobic Surfaces

The term *wettability* refers to the interaction between liquids and surfaces. In this section, the behavior of water molecules is studied via surface interaction. In the human body, each cell membrane with a thickness of 8 nm functions as a traffic controller between the inside and outside of the cell. It is called selective permeability [40] in proteins, ions, and other

20

biomolecules. The cell membrane is formed by a lipid bilayer. The first artificial cell membrane was made by Langmuir in 1917 [40], by using benzene as a solvent to add phospholipid into the water. The phospholipid may be distinguished from hydrophilic heads and hydrophobic tails by its appearance. The position of the head and the tail of the phospholipid is directed toward the water and against the water respectively, as shown in Figure 3.4.

Careful examination of the cell membrane reveals that there are two layers: The outer layer is the hydrophilic layer and the inner layer is the hydrophobic layer. The hydrophilic and hydrophobic behaviors of the cell membrane are based on a molecular structure. The head of the phospolipid consists of a polar group which attracts water molecules, and the tail of the phospolipid consists of a non-polar group which repels water molecules.
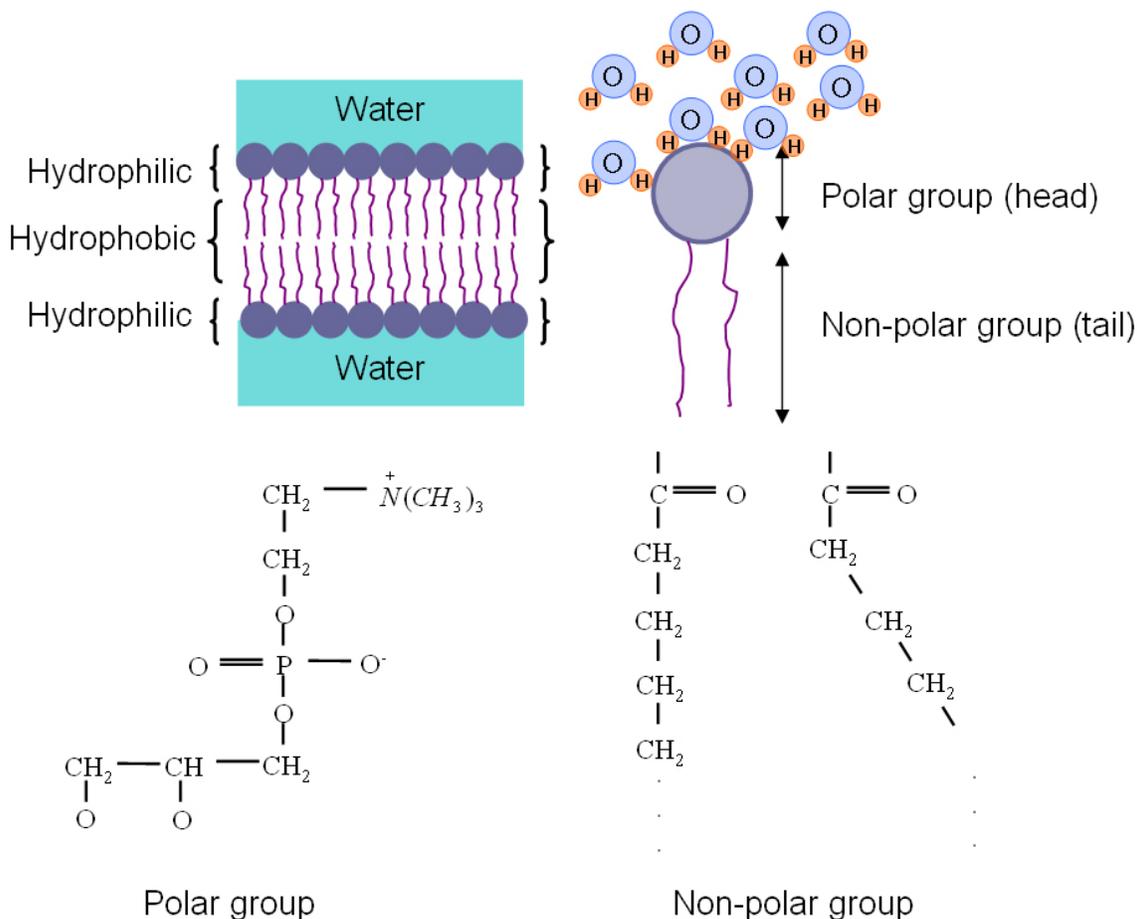
Figure 3.4. Schematic diagram of cell membrane and its phospholipid.

There is an important rule for molecular interaction in water. In water molecules, oxygen has a slightly negative property, while hydrogen has a slightly positive property. The polar molecules of the solid surfaces can be joined to water molecules by a hydrogen bond, which causes the water to spread on the solid surface. The surface energy increases with the larger, attractive force. A substrate with high surface energy will offer an advantage of more spread to a given liquid. Hydrophilic layers are named as the layers that attract water molecules. On the other hand, non-polar molecules repel liquid molecules, and thus are called hydrophobic layers, due to the low surface energy.

Angle = 12.28
Base Width = 6.7971

Angle = 106.40
Base Width = 2.1865

(a)   (b)
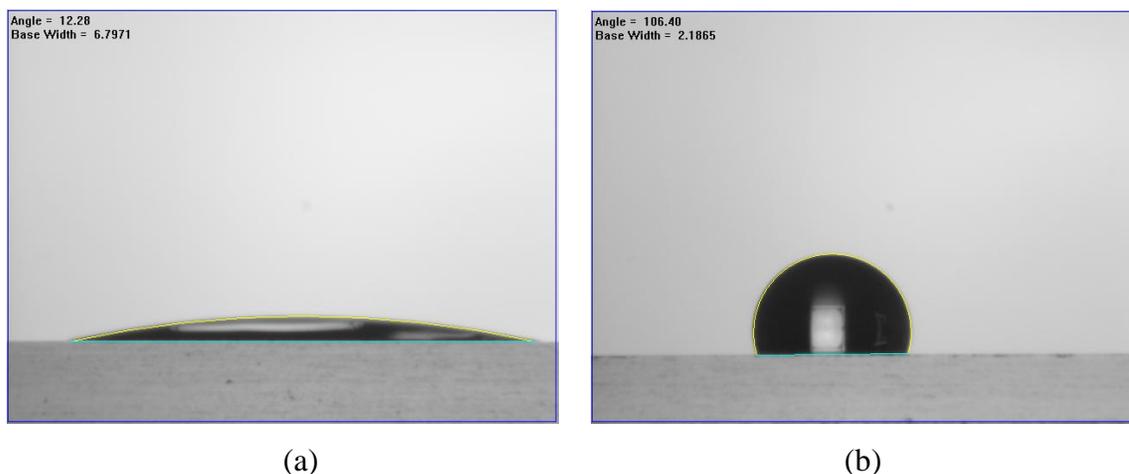
Figure 3.5. Surface energy difference: (a) hydrophilic surface and (b) hydrophobic surface.

In this sense, it may be thought that hydrophilic and hydrophobic properties are determined by different surface energies. Generally, a hydrophilic surface has a low contact angle (less than 90 degrees) and a hydrophobic surface has a high contact angle (greater than 90 degrees) [39]. Most metals exhibit hydrophilic property, because their surfaces have high energy (500 to 5000 erg/cm^2) which consists of covalent bonding. On the other hand, most polymers have hydrophobic property, due to low surface energy (50 erg/cm^2) which consists of van der Waals bonding [38]. Figure 3.5 shows examples of hydrophilic and hydrophobic surfaces. In

the case of a water droplet on the glass, the contact angle is 12.28°, as shown in Figure 3.5 (a). The contact angle of a water droplet on the cyclized perfluoro polymer (CPFP), Cytop® from Asahi Glass Co. (Tokyo, Japan), shows 106.40° as shown in Figure 3.5 (b).

Chemically, since the surface of glass has covalent bonding, it can be estimated that it has high surface energy, due to low contact angle. The CPFP consists of the -CF_3 group, which has van der Waals bonding; therefore, it can be considered to have low surface energy. Water will spread on high energy surfaces, and thus the water will form a sphere on low energy surfaces.

Wettability is an importance parameter in microfluidic applications. Microfluidic channels can be created by combining hydrophilic and hydrophobic surfaces, and thus water flow inside the microfluidic channels can be manipulated [36].

3.4 Experimental Verification of Surface Properties

3.4.1 Device Preparation

In order to characterize the surface energy of different solid surfaces, a contact angle goniometer (First Ten Ångstrom 125) was used for measuring contact angles.

Figure 3.6. Calibration set for the calibration of contact angle measurement. The structure imitates the contact angles of 15.9°, 90°, and 39.6° from the left.

23

Before measuring contact angles, a calibration is required, because the contact angle goniometer performs image processing by means of digital camera magnification. The simplest way to calibrate the system is to measure and compare contact angles of known shapes by placing a calibration set as shown in Figure 3.6.

First, the surface energy of polyemethyl methacrylate (PMMA, $75 \times 25 \times 5$ mm) was measured as a sample polymer substrate. Another polymer substrate CPFP coated slide glass was also prepared. Cytop® (CTL-809M) was spin-coated at 2000 rpm for 1 minute and cured at 180°C for 30 minutes to form the CPFP coated slide glass. Metal substrate was prepared by depositing 2,000 Å of aluminum on a slide glass, using an e-beam evaporator.

Table 3.1. Surface tension of different liquids.

Materials	Water	Chloroform	IPA
Surface tension [dyne/cm]	72.8	27.15	21.7

Several sample liquids such as DI water, chloroform, and isopropyl alcohol (IPA) were used for extrapolating the surface energy. Each liquid exhibited its own surface tension, as shown in Table 3.1.

3.4.2 Experimental Results

Based on the description of surface energy in section 3.3, experiments were carried out to obtain critical surface tension values of various solid surfaces by the Zisman model. Table 3.2 summarizes the measured contact angles of water, chloroform, and IPA on various surfaces.

Table 3.2 Contact angle data for different solid surfaces.

Materials	PMMA	Cytop	Aluminum
Water	69.23°	106.4°	63.21°
Chloroform	5.44°	41.37°	4.46°
IPA	3.87°	36.92°	3.71°
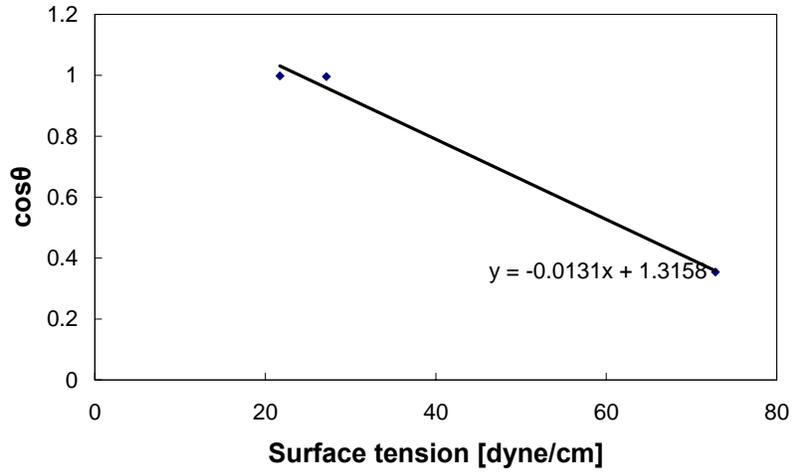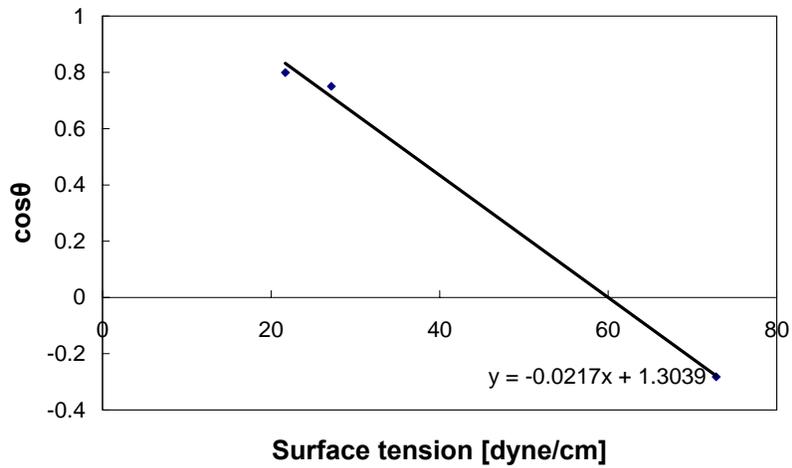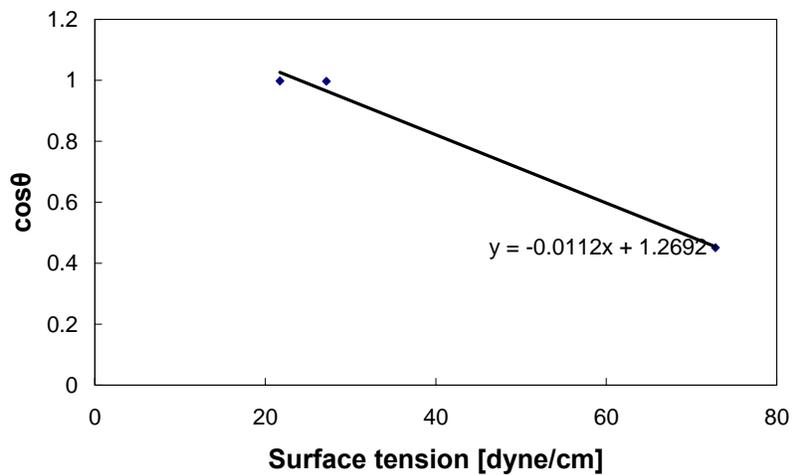
Figure 3.7. Surface tension versus contact angle curves of: (a) PMMA, (b) Cytop®, and (c) aluminum. The extrapolated curves are used to determine the surface energy using the Zisman model.

Using the measured data, surface tension versus contact angle curves are extrapolated to derive the surface energy values of each surface. The extrapolated curves are shown in Figure 3.7.

Critical surface tension for various solid surfaces can be derived from Figure 3.8 by observing the point where the cosine value of the contact angle is equal to unity. The obtained critical surface tension values are summarized in Table 3.3.

Table 3.3. Critical surface tension (CST) data of different solid surfaces.

Materials	PMMA	Cytop®	Aluminum
CST (dyne/cm)	24.11	14	24.04

As expected, Cytop® has the lowest surface energy value, and it can be considered a hydrophobic surface, which is true. On the other hand, the Zisman model has a limitation to measure the surface energy, because the Zisman model may be applicable to estimate low surface energy materials [39].

3.5 Conclusions

In this chapter, the wettablility of different surfaces were analyzed and characterized by using contact angles. The Zisman method was used as a tool for determining the surface energy. Contact angles were observed from the contact angle goniometer. According to the contact angle measurement results obtained, it can be inferred that in the presence of surface energy by the Zisman plot, it is still difficult to predict the exact surface properties due to contaminants or molecular imperfection. In experiment, Cytop® showed a strong hydrophobic surface.

CHAPTER 4. ELECTROWETTING

4.1 Introduction

Electrocapillarity experiments may be traced back to an experiment that was conducted by Gabriel Lippmann in 1875, using mercury in contact with an electrolyte, where a voltage was applied as shown in Figure 4.1 (a) [36]. In the early 1990s, Berge *et al.* utilized a thin insulator to separate the conductive liquid and the metallic layer to prevent a electrolysis problem, as shown in Figure 4.1 (b) [41].

Berge *et al.* used 12 μm thickness polyethylene film as an insulator ($\varepsilon_r \sim 3$) and conductive water without a surfactant. In contrast to Lippmann's experiment, Berge's experiment required a higher voltage, approximately 170 V [41]. Due to the insulating layer, there was no electrolysis problem allowing action as a capacitor which accumulated electric charges. With the applied potential, the contact angle of the conductive liquid was changed, which was referenced as *electrowetting*.

Wetting generally means the interaction of a liquid on a given solid [1]. Each solid surface has its own distinct, wetting value. A hydrophilic surface provides more wetting than a hydrophobic surface. In order to control the shape of the liquid droplet, the solid surface must be controlled, and hence the surface energy of the solid should be controlled. Yet there are several ways to control surface energy, some of which include varying the temperature, the chemical and topographical structure of the surface, and so on [1].

In miniaturized fluidic systems, electrowetting, as a means of electrical surface modification, represents one of the best methods to control the liquid droplet by controlling surface energy. Electrowetting is more efficient than any chemical surface modification methods, since hydrophilic and hydrophobic surface properties have a static nature [42].
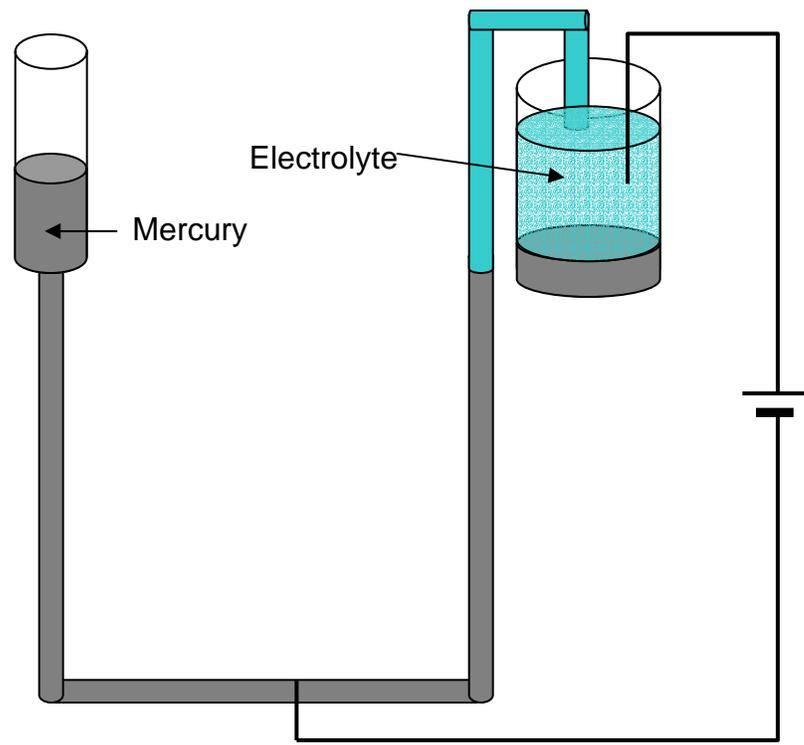
(a)
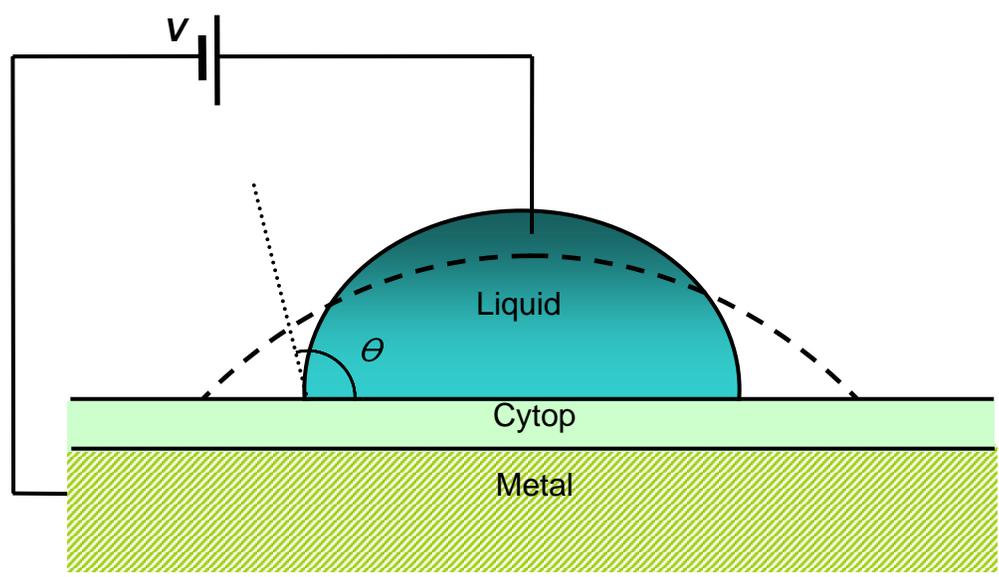
(b)

Figure 4.1. Electrocapillary and electrowetting experiments: (a) the concept of Lippmann's electrocapillary experiment [36] and (b) the setup for electrowetting experiment [41].

4.2 Electrowetting Dynamics

4.2.1 Principle of Electrowetting

The theory of electrowetting presents a unified and consistent approach to determining the overall microscopic behavior of liquid droplet edges, subject to various external influences. The specialized treatment of electrowetting employs three models to determine a system's response. These are: the thermodynamic and electrochemical approach, energy minimization approach, and electromechanical approach [36]. Although those different approaches describe electrowetting phenomena, Berge *et al.* proposed a general theory that accounts for electric potential, surface tension, and contact angle, as shown in Figure 4.2. The relationship of those parameters can be expressed by

$$\cos\theta = \cos\theta_0 + \frac{\varepsilon_0 \varepsilon_r}{2d\gamma_{LV}} V^2, \qquad (4.1)$$

where θ_0 is the initial contact angle, d is thickness of the dielectric layer, ε_r is the dielectric constant, ε_0 is the dielectric permittivity in free space, γ_{LV} is the surface tension of the liquid and vapor interface, and V is the electric voltage as shown in Figure 4.2 [41-43].
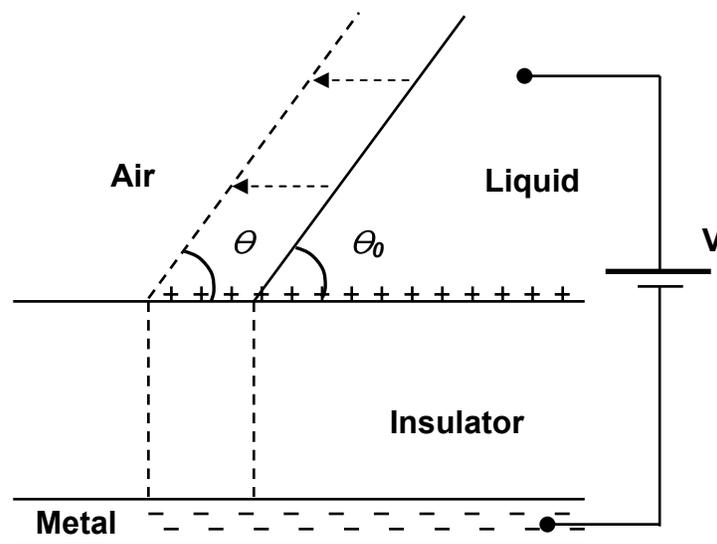
Figure 4.2. Schematic diagram of electrowetting. The contact line is moving with the applied electric potential [36].

Figure 4.3 shows the traditional electrowetting phenomena. The thickness of the dielectric layer *d* should be as small as possible if liquid spreading is to occur, but it is easy to break down the dielectric layer. In theory, the cosine value of contact angle (cos θ) is proportional to the square of the applied voltage. Above a certain voltage, however, saturation of the contact angle occurs.

| (a) | (b) |
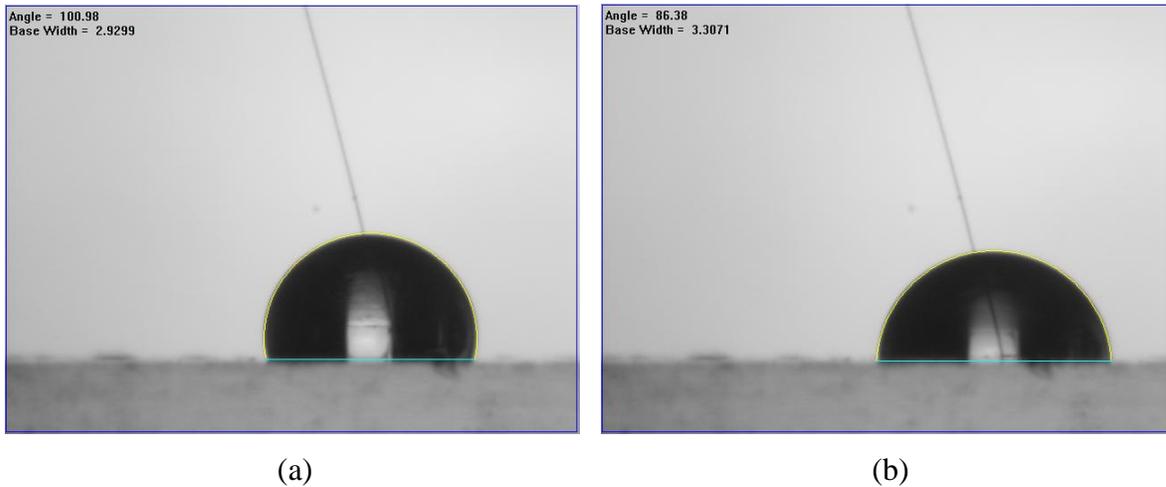
Figure 4.3. Contact angle change of the 5 μl of 1% KCl solution by electric potential: (a) 0 V and (b) 110 V, respectively.

4.2.2 Device Preparation

Figure 4.4 illustrates a contact angle measurement system setup for electrowetting. A contact angle measurement system can also be used to capture images by digital camera (FTA32 Frame grabber, First Ten Ångstrom, Portsmouth, Virginia) and to analyze the liquid droplet's dimension by image processing software (FTA 32 Video Program). A DC power supply (Keithley model 248, Keithley, Cleveland, Ohio) can also be added to apply an electric potential on the liquid droplet. Aluminum film and insulator layers coated a slide glass substrate, which was placed on the stage and connected to the power supply. The aluminum film had thickness of 200 nm and was deposited by e-beam evaporation. The insulator layer was conformed to coat a

layer of 5 µm-thick Parylene and a layer of 1 µm-thick Cytop®. The Cytop® layer, formed by

spin coating (2000 rpm for 1 minute), and was cured at 120°C for 30 minutes. The conductive

liquid was a mixture of 1% potassium chloride (KCl) in DI water. A thin, gold wire with 20 µm

diameter was connected into the 5 µl of 1% KCl solution.

(a)

(b)
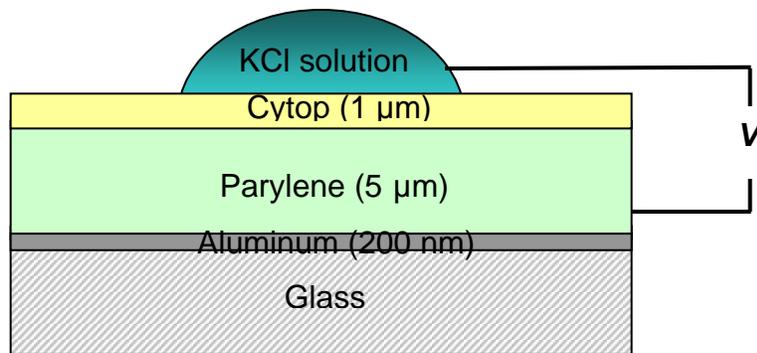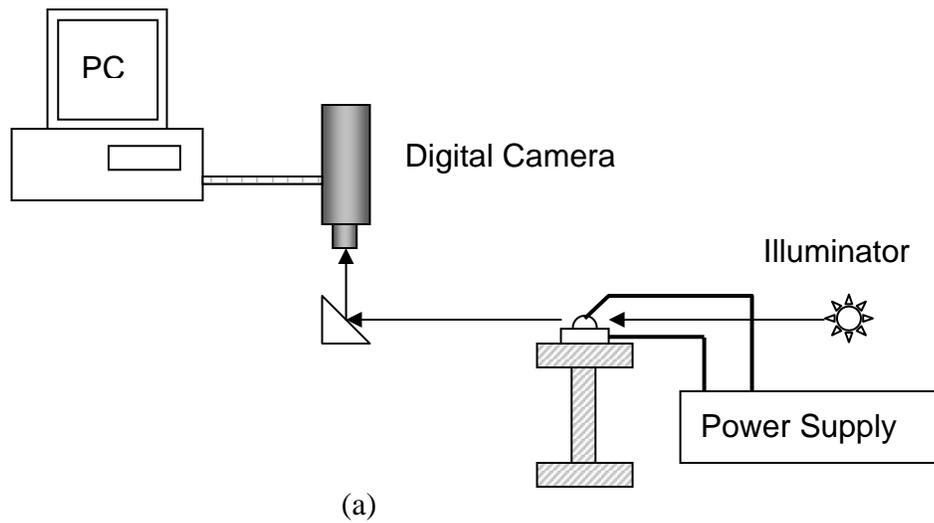
Figure 4.4. Electrowetting experiments: (a) the electrowetting measurement system and (b) a test device.

4.2.3 Experimental Results

Figure 4.5 shows the pictures of liquid droplets on the dielectric layer with a continuous change voltage from 0 V ~ 120 V, applied by a DC power supply.

0 V / 100.98°	40 V / 98.76°	50 V / 98.56°
60 V / 96.29°	70 V / 94.67°	80 V /92.21°
90 V / 91.90°	100 V / 89.13°	110 V / 86.38°
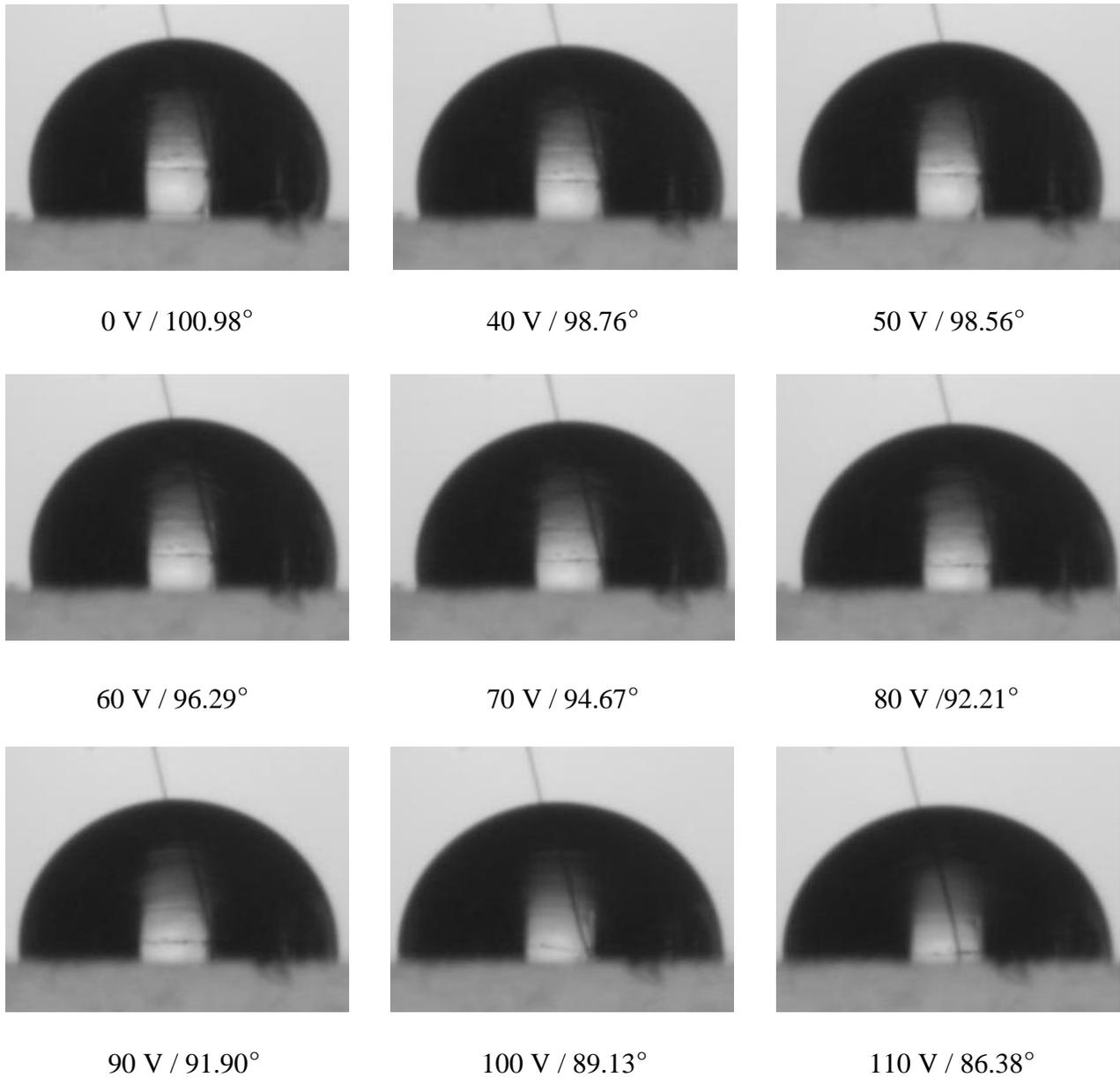
Figure 4.5. Electrowetting experimental results with measured contact angles for various voltages.
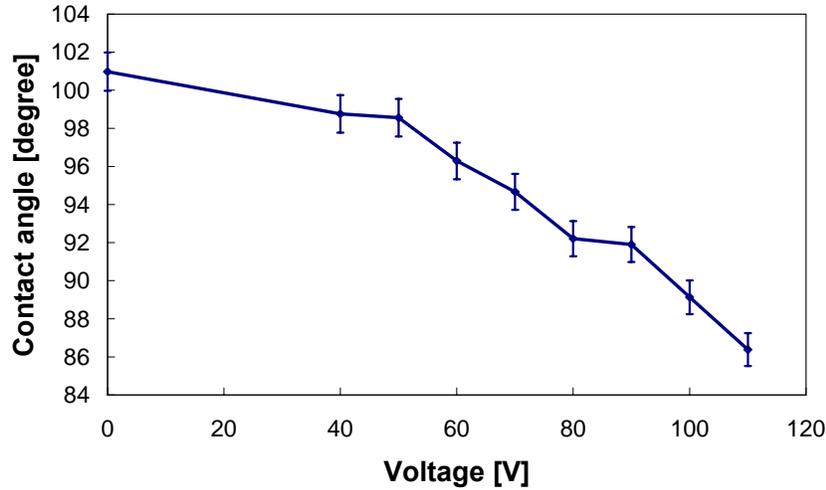
Figure 4.6. Measured contact angle versus the applied voltage. The conductive liquid droplet was 5 μl of 1% KCl solution.

In Figure 4.6, the voltage-contact angle curve of 5 μl volume of 1% KCl solution with the increased voltage is shown, based on the measurement in Figure 4.5. The contact angle decreased as the voltage increased from 0 V to 120 V. Saturation of the contact angle was observed for voltages higher than 120 V.

4.3 Competitive Electrowetting

4.3.1 Principle of Competitive Electrowetting

Recent developments in electrowetting applications have focused on actuating one-phase liquids, such as aqueous solutions or liquid metals [44-46]. In 2000, W. Göpel *et al.* provided an excellent overview of competitive electrowetting that had contact angle variation in a submersed decane ($C_{10}H_{22}$) droplet inside water [47]. Figure 4.7 illustrates an experimental setup for competitive electrowetting. By applying electric voltage, the contact angle change of decane was observed. W. Göpel *et al.* considered the interfacial tension between water and polymers and related it to electric field:

$$\Delta\gamma = \frac{1}{2} \cdot \frac{\varepsilon_0 \varepsilon_r}{d} \cdot (V - V_0)^2 , \qquad (4.2)$$

where d is the thickness of insulator layer, ε_0 is the electric permittivity in free space, ε_r is the relative permittivity, V is the applied voltage, V_0 is the initial voltage, and $\Delta\gamma$ is the interfacial tension [47].
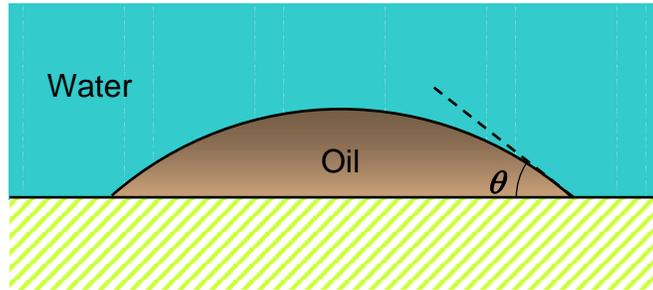
(a)
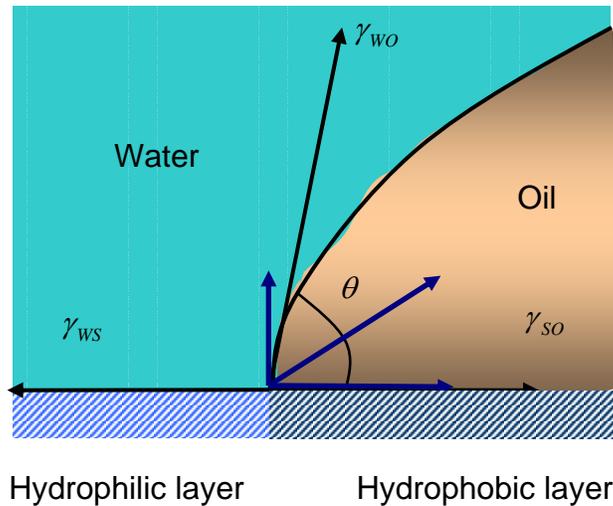
(b)

Figure 4.7. Concept of competitive electrowetting: (a) experimental setup and (b) schematic diagram of competitive electrowetting.

4.3.2 Device Preparation

Before the experimental study of the competitive electrowetting phenomena, test devices were prepared and materials were chosen, using the same glass slide shown in section 4.2.2, with a thin aluminum layer covered with Parylene and Cytop layers. A PDMS (polydimethylsiloxane)

layer was prepared by casting a mixture of PDMS prepolymer (Sylgard 184) and a curing agent in a 10:1 ratio. The PDMS layer was cured and then cut to a rectangular shape in a 20 mm × 20 mm size, with a 10 mm × 10 mm window. The prepared PDMS layer then was placed on the electrowetting substrate to form a chamber to confine the electrolyte solution.

An aqueous solution of 1% KCl was poured into the PDMS chamber, and silicone oil (Dow Corning's 200 fluid 350 CST) was submersed into the KCl solution. We chose the silicone oil because density of the silicone oil is 0.97 g/cm^3 which is similar to density of water. The aluminum layer was connected to a DC power supply (Keithley model 248) and a 20 μm-thick gold wire was connected directly to the water.

4.3.3 Experimental Results

The test device was put under the contact angle measurement system, as described in section 4.2.2. The silicone oil volume was 5 μl. For a direct demonstration of competitive electrowetting, the contact angle of the oil droplet was immersed in the KCl aqueous solution was changed by the electric voltage.
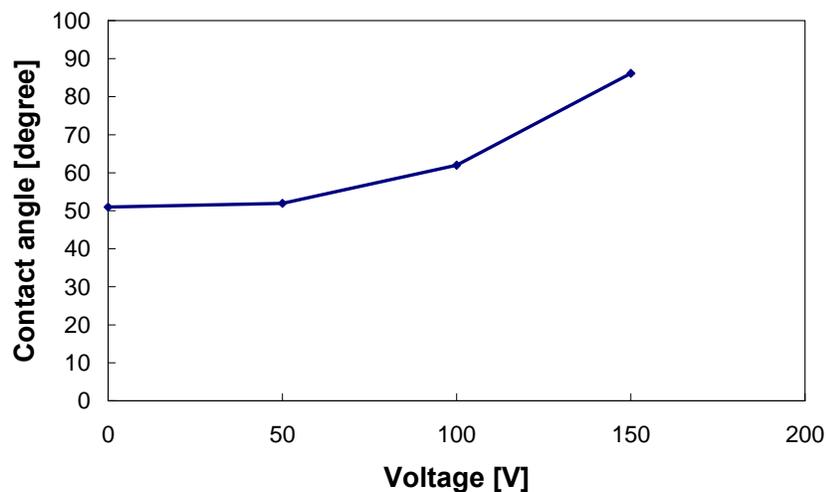
Figure 4.8. Measured contact angle of the 5 μl of silicone oil droplet inside 1% KCl solution.
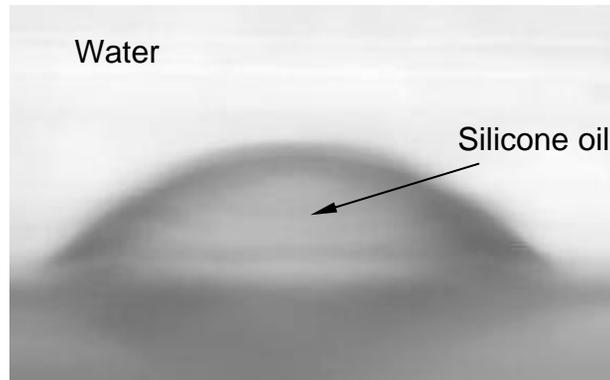
(a)

(b)

(c)

Figure 4.9. Experiment results of competitive electrowetting: (a) at 50 V; (b) at 100 V, and (c) at 150 V.

Figures 4.8 and 4.9 show the voltage-induced contribution of KCl aqueous solution to the contact angle of the oil droplet dimension. The experimental results demonstrate that the contact angle of silicone oil increases as the applied voltage increases.

4.4 Conclusions

Electrowetting principles and phenomena were studied in this chapter. An aqueous electrolyte droplet on a hydrophobic surface with an electrode underneath underwent electrowetting in response to an applied electric potential to the electrode. As the voltage increased, the contact angle of the droplet decreased, showing the electrowetting effect. It was observed that the contact angle of the aqueous droplet saturated when the applied voltage was higher than 120 V.

In addition, competitive electrowetting was studied and experimentally investigated. An immiscible liquid droplet, surrounded by an aqueous solution, was tested to verify competitive electrowetting phenomena. Silicone oil was chosen as the immiscible liquid droplet for the experiments. The measured results clearly demonstrated competitive electrowetting of the silicone oil droplet in 1% potassium chloride solution. The contact angle of a submersed silicone oil droplet increased with applied voltage, as the testing solid surface became hydrophilic and attracted the aqueous solution.

The shape and the contact angle of a submersed, non-polar, liquid droplet in aqueous solution can be controlled by an applied electric potential, which enables the submersed liquid droplet to act as a variable focal length liquid lens. In the next chapter, design and characterization of a liquid lens will be addressed.

CHAPTER 5. A LIQUID LENS BASED ON ELECTROWETTING

5.1 Introduction

It is obvious that electrowetting is a versatile tool to achieve miniaturized fluid systems, as demonstrated in section 4.2. This can be explained in a number of different applications. In addition to the general methods, some specialized techniques are also required, such as competitive electrowetting, the concept of wetting in two phase liquids. In this chapter the liquid lens design is further developed, which enables integration onto a lab-on-a-chip system. The planar liquid lens design is presented in section 5.2.2. In addition, the optical properties of the liquid lens are also characterized under different size diameters (section 5.3.3).

5.2 Design and Fabrication

5.2.1 Design Considerations

The liquid lens developed in this work is based on a planar and on-plane electrode structure. Thus, electrodes can be arranged on the same plane without a vertical and out-of-plane wall electrode, so that the liquid lens dimensions can flexibly be designed for integrated lab-on-a-chip systems. However, this planar liquid lens design has a confinement problem. To prevent this, a ring type electrode shown in Figure 5.1 is used for confining a silicone oil droplet. The pre-charged outer ring electrode works as a hydrophilic layer using electrowetting instead of a wall structure. By applying an electric potential on the ring electrode, its surface property is changed from hydrophobic to hydrophilic, so that water is attracted on the ring electrode and oil is confined.
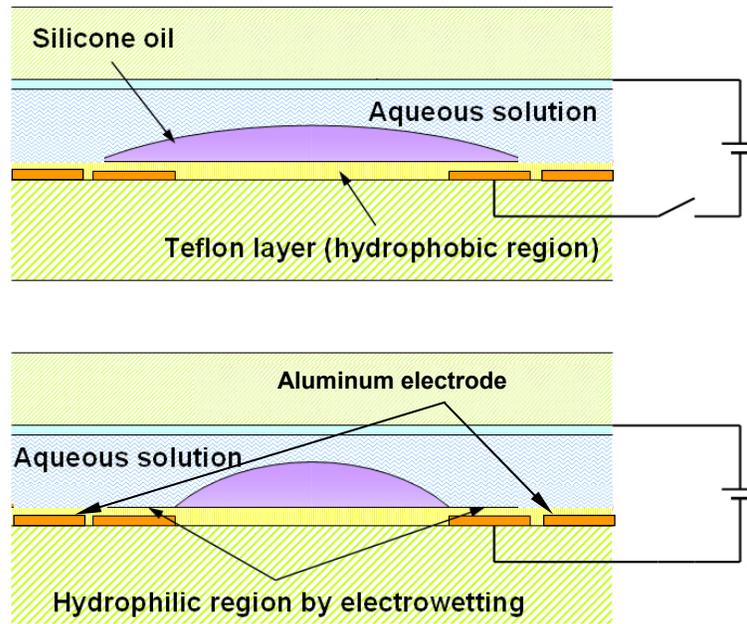
Figure 5.1. Schematic diagram of the liquid lens design. The electrodes are 200 nm-thick aluminum and the insulator is a 5 µm-thick Parylene layer with a 1 µm-thick Cytop® layer.

5.2.2 Device Design

The required geometry for a planar liquid lens is two separated ring electrodes with a small gap between the electrodes. The outer ring electrode should be separated from inner electrode as an insulator between the two electrodes. A detailed design is shown in Figure 5.2.

The approach used in this work was to control surface properties electrically. Originally, the Cytop-coated surface has a hydrophobic property, but is temporarily modified into a hydrophilic layer, using electrowetting. This helps pull water molecules towards the electrode area, and hence oil is confined within the patterned electrodes.

Oil confinement is one of the key issues because the density of silicone oil is 0.97 g/cm^3, that is, slightly smaller than water. Without a hydrophilic pattern, the oil droplet will either float or get dispersed. However, the pre-charged electrodes attract water because electric potential may affect changes on hydrophobic surface as hydrophilic surface. On the other hand, water on

39

discharged electrodes is quite unstable, since the water is repelled by the hydrophobic surface. Electrodes should be charged before submersing the silicone oil droplet inside water.
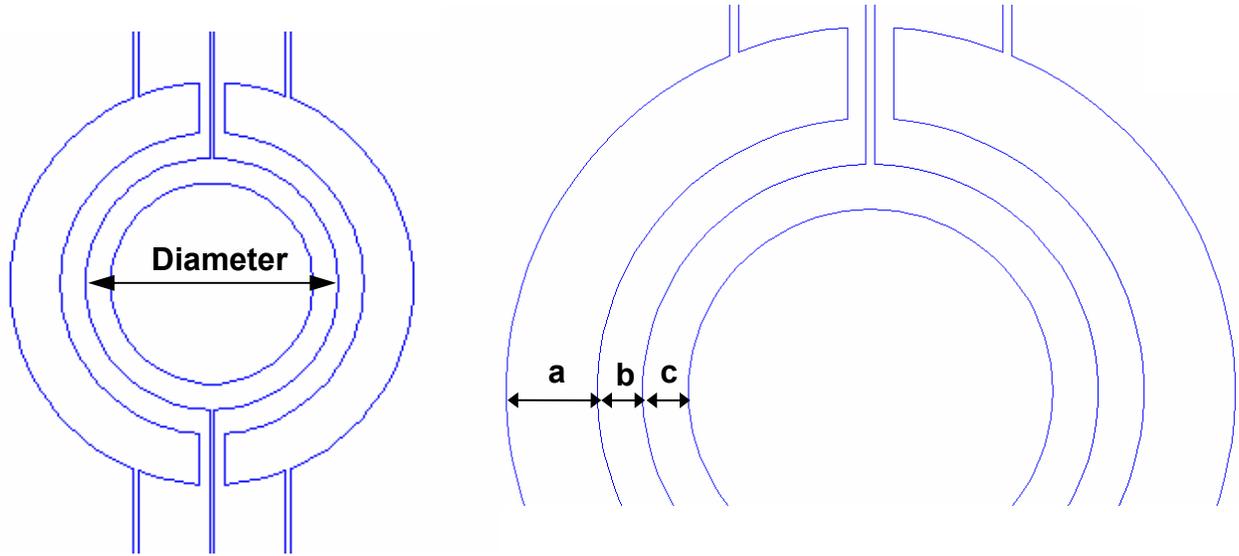
Lens Diameter	a	b	c
2 mm	200 μm	100 μm	100 μm
3 mm	200 μm	100 μm	200 μm
4 mm	200 μm	100 μm	200 μm

Figure 5.2. Design and dimensions of ring electrodes.

5.2.3 Fabrication

Figure 5.3 shows a schematic diagram of the liquid lens. The device described above was fabricated by standard microfabrication process. A glass substrate was immersed in acetone for 30 minutes, and rinsed with methanol and DI water. Water residues were blown out by nitrogen gas and the slide glass was heated up on a hot plate at 200°C for 20 minutes. 200 nm-thick aluminum was deposited by e-beam evaporation, which allows accurate thickness control and conformal coating.
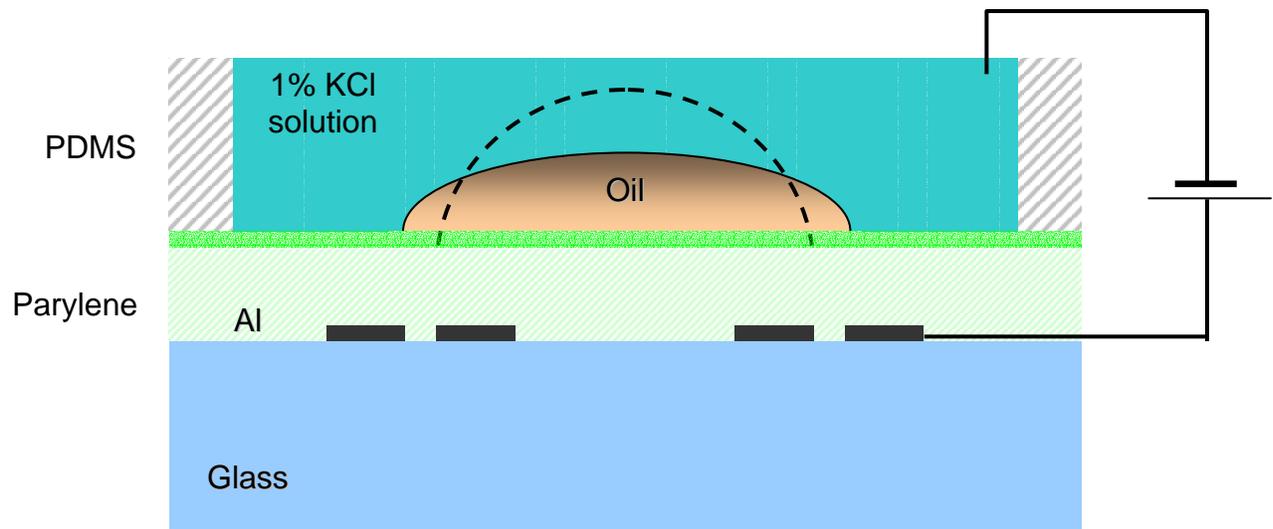
(a)
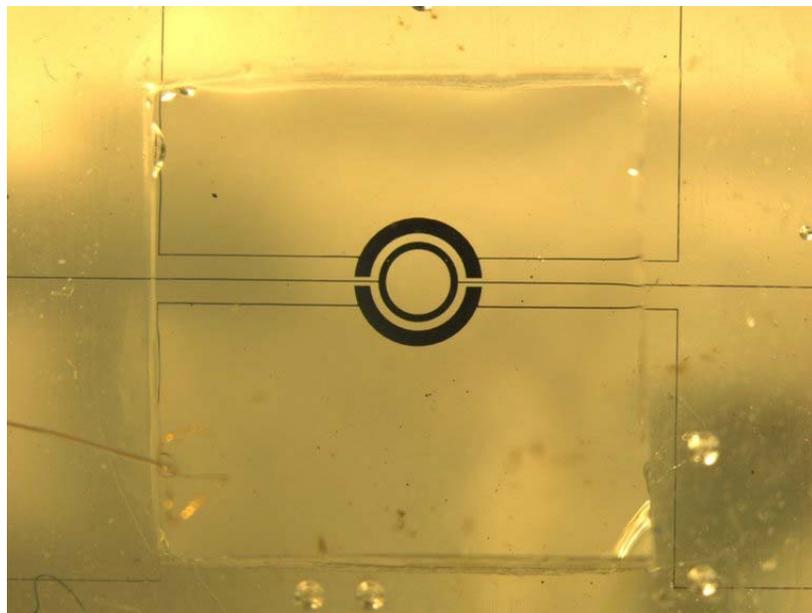
(b)

Figure 5.3. Planar liquid microlens: (a) a schematic illustration of the cross-section view and (b) a photograph of the fabricated structure.

The patterned aluminum electrodes were fabricated by a photolithography technique. A positive photoresist (Microposit S1813, Shipley) was coated, using a spin coater at 2900 rpm for 47 seconds with a 500 rpm spread cycle for 10 seconds. The substrate was soft-baked at 110°C for 2 minutes on a hotplate. The substrate was then exposed by UV exposure (Quintel) at a wavelength of 365 nm for 11 seconds, using a contact mode.

After that, the substrate was developed by developer (Microposit Developer 354, Shipley) for 40 seconds and rinsed with DI water. After developing, the substrate was hard baked on a hotplate at 110°C for 5 minutes.

For aluminum etching, an aluminum etchant, a mixture of 90% phosphoric acid, 5% nitric acid, and 5% DI water was prepared and used. The 200 nm-thick aluminum layer was etched for 120 seconds and then rinsed with DI water. The photoresist was finally etched away in the acetone solution.

Next, a 5 μm-thick Parylene layer deposited on the patterned aluminum electrodes was followed by a 1 μm-thick Cytop layer. The substrate baked at 120°C for 30 minutes on a hotplate.

A PDMS layer was prepared, using PDMS (Dow Corning's Sylgrad 184) resin, mixed with a curing agent at a ratio of 10:1 and then cured. The PDMS layer was cut to a rectangular shape in 20 mm × 20 mm with a 10 mm × 10 mm window.

Subsequently, the PDMS structure was placed on the substrate, forming a chamber, and a 1% KCl aqueous solution was poured into the PDMS chamber. The bottom aluminum electrode was connected to the DC power supply (Keithley model 248) and then a 20 μm-thick gold wire was connected to the water.

The adequate volume of a silicone oil (Dow Corning's 200 fluid, 350 CST) droplet was submersed into the water by a micropippet (Eppendorf, Hamburg, Germany) and covered with a cover glass. Figure 5.4 shows the fabrication of a liquid lens for testing.
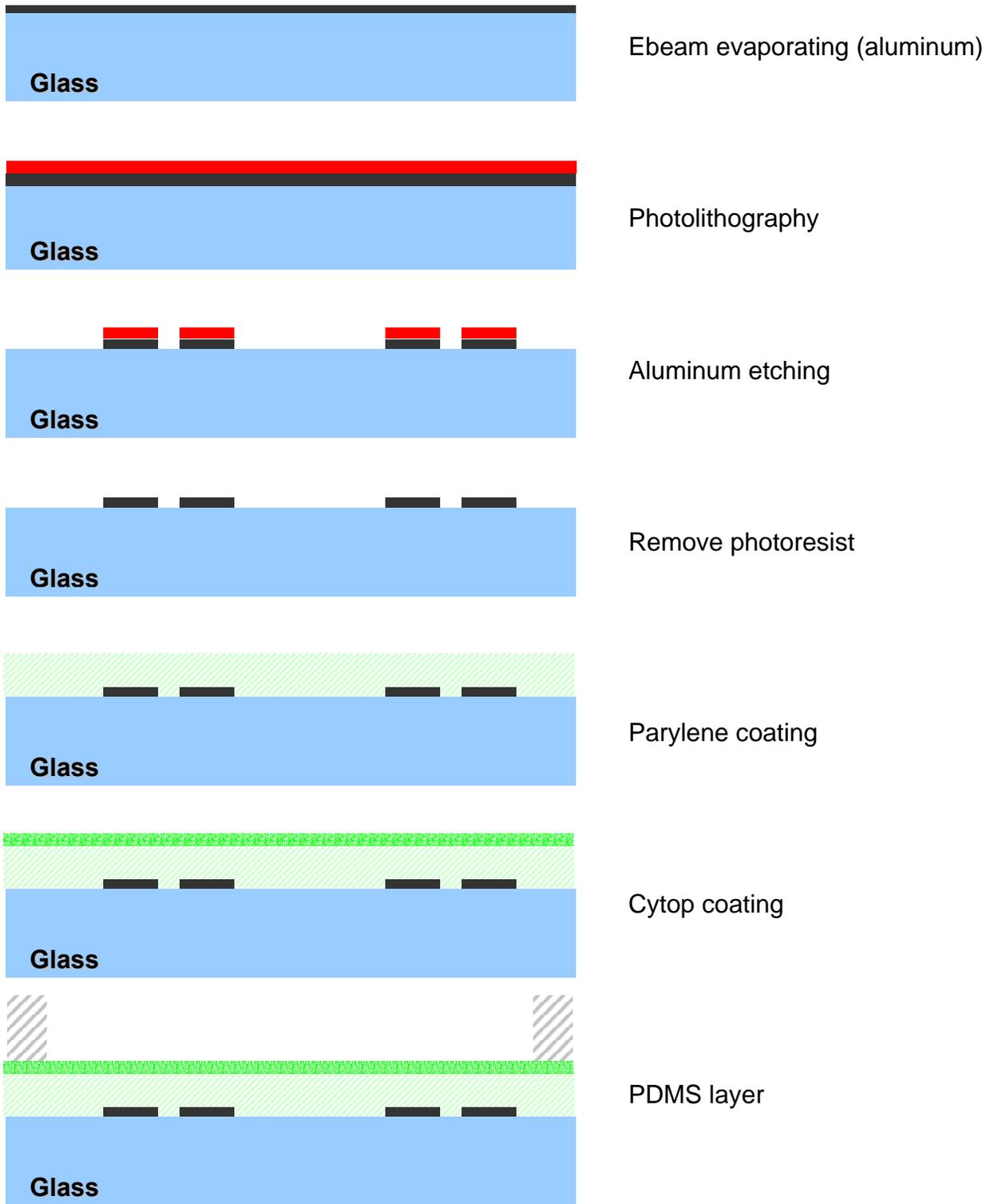
Figure 5.4. Fabrication steps of the liquid lens.

5.3 A Liquid Lens Test Results

5.3.1 Focal Length Measurement

To examine the optical characteristics of the liquid lens, the focal length was measured at different electric voltages. Although there are several ways to obtain the focal length of an optical lens, the magnification of the object can be used for the focal length measurement because the magnification depends on focal length of the lens. When an object is placed within the focal length of a convex lens, a virtual image will be created as shown in Figure 5.5.

The lens formula for the case in Figure 5.5 will be:

$$\frac{1}{f} = \frac{1}{d_O} - \frac{1}{d_I}, \tag{5.1}$$

where f is the focal length, d_O is the distance from the lens to the object, and d_I is the distance from the lens to the image. The ratio between d_O and d_I is equal to the ratio between the object size h_O and the image size h_I. Magnification m can be defined by

$$m = \frac{d_I}{d_O} = \frac{h_I}{h_O}. \tag{5.2}$$
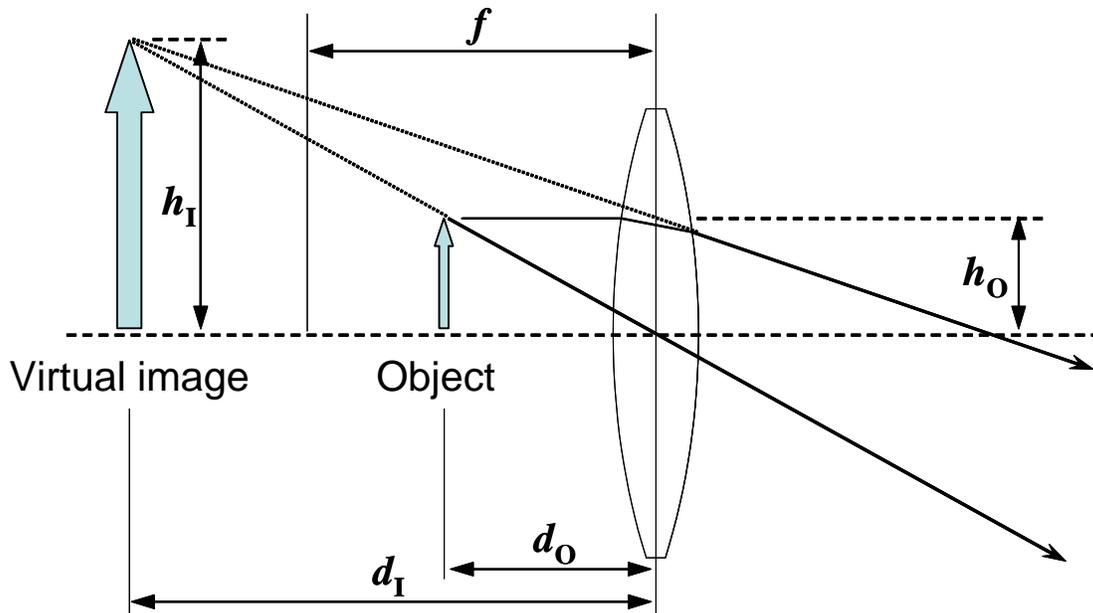
Figure 5.5. Schematic diagram of focal length, virtual image, and magnification.

Putting (5.1) into (5.2) by eliminating d_I:

$$m = \frac{f}{f - d_o} \, .$$

<div align="right">(5.3)</div>

If d_O and m are measured, therefore, f can be determined.

Using a stereomicroscope (Leica DFC Camera MZ 16A), the magnification m was measured from the ratio of projected images, and the distance between the liquid lens and the object d_O was also measured by a micromanipulator (MM Model 2525), as illustrated in Figure 5.6.
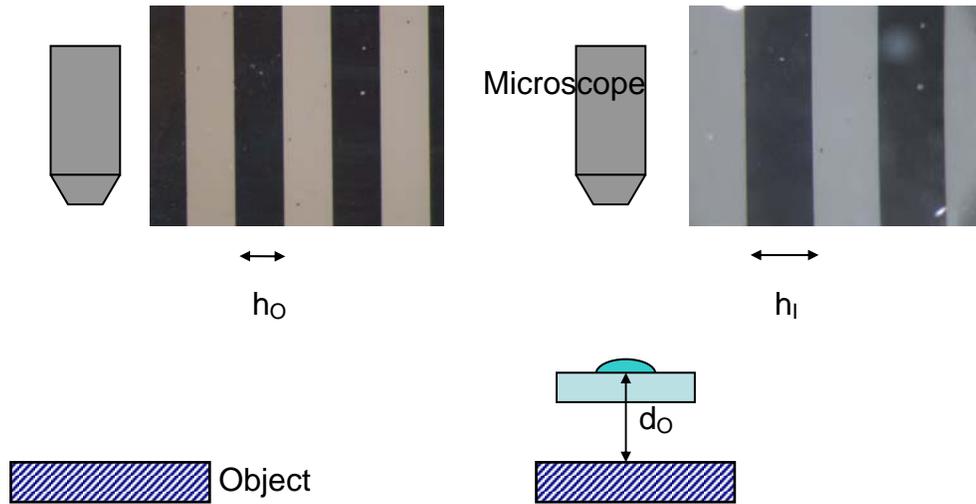
Figure 5.6. Schematic diagram of measured magnification (m), and the distance between the lens and the object (d_O).

The measurement method of the magnification and the distance to the object is illustrated in Figure 5.6. First, the object was placed under the stereomicroscope and focused without the liquid lens. The focused image was taken and the size of the object was measured. Then, the liquid lens was placed above the object. The distance between the liquid lens and the object was adjusted to obtain a focused and magnified image. By comparing the magnified image and the previous image, the magnification was determined. At the same time, d_O was also measured.

5.3.2 The Effect of Electric Voltage

The focal length was measured as described in the previous section. Due to the competitive electrowetting effect, the focal length of the liquid droplet was varied by the applied electric potentials. The calculated and measured focal lengths are shown in Figure 5.7 for the liquid lens whose diameter was 3 mm. The volume of silicone oil was about 2.8 µl and the refractive index of the oil and the 1% KCl solution were 1.4 and 1.49, respectively.
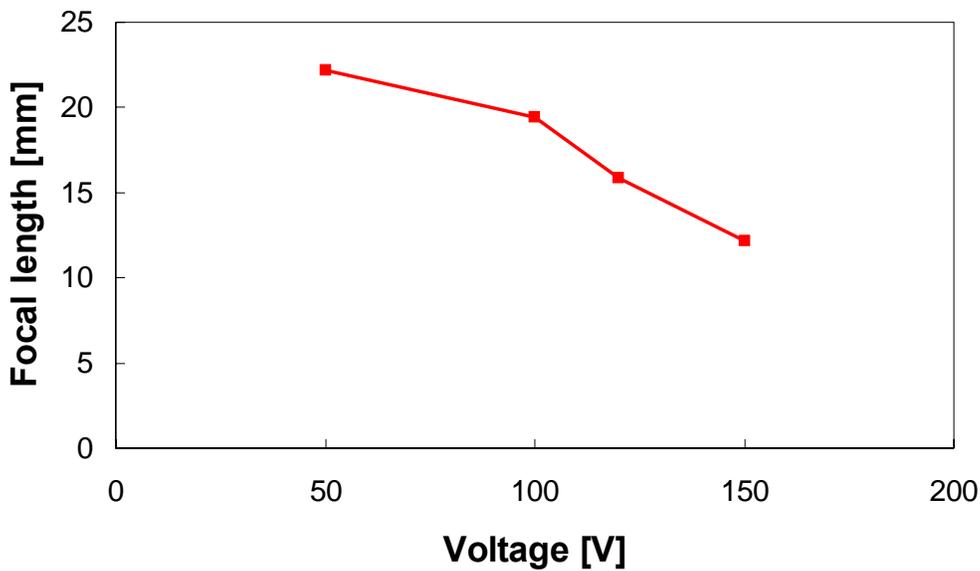
Figure 5.7. Varying the focal length of the 3mm diameter liquid lens. The applied potentials were from 50 V to 150 V. The focal length values were determined by measuring the magnification and the objective distance.

As expected, the contact angles of the oil droplet were proportional to the applied voltages, and the focal lengths of the oil lens were related to those applied voltages as shown in Figure 5.7. From the experimental results, the focal lengths of the liquid lens were varied from 12.2 mm (at 150 V) to 22.2 mm (at 50 V). Figure 5.8 shows the image qualities of the liquid lens. The lines were magnified at higher electric potentials as demonstrated in Figure 5.8.

(a)

(b)

100 µm
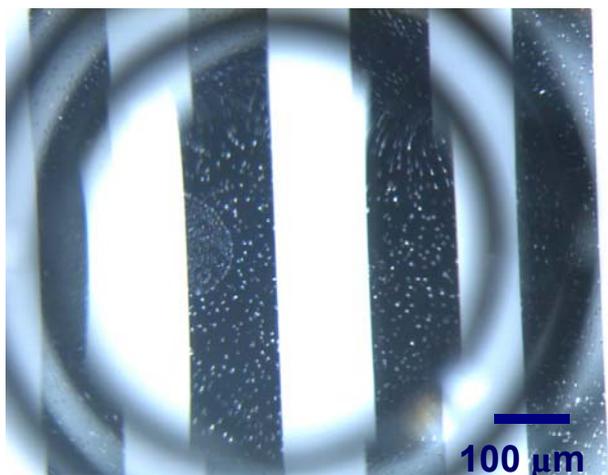
(c)

Figure 5.8. Demonstrated liquid lens at different applied voltages: (a) at 50 V; (b) at 100 V, and (c) 150 V.

5.3.3 The Effect of Different Lens Diameter

The focal lengths of each liquid lens were also measured for the different diameters of the liquid lens: 2 mm, 3 mm, and 4 mm. The results are shown in Figure 5.9.
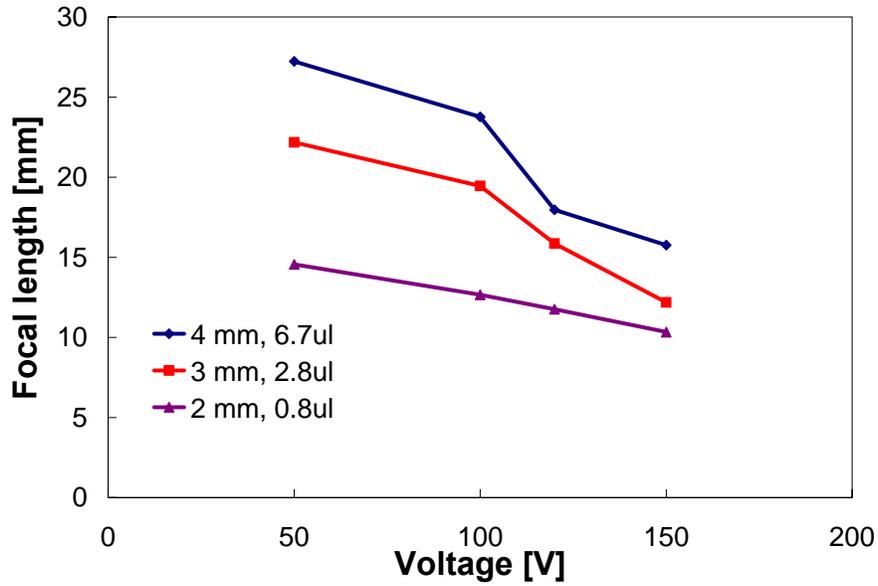
Figure 5.9. Effect of the lens diameter on focal length of the liquid lens.
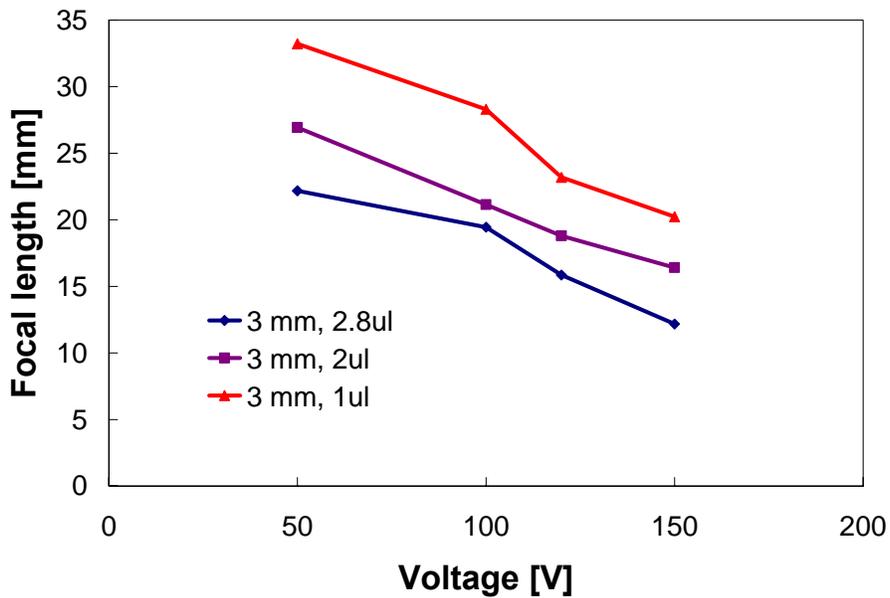
Figure 5.10. Effect of the liquid volume on focal length of the liquid lens.

48

The observed decrease of the focal length was caused by different diameters of the liquid lens. For the 2 mm lens, the focal length of 10.3 mm was also achieved at the applied potential of 150 V. Figure 5.10 shows the focal length of each volume of lens with 3 mm diameter. The smaller volume of lens showed the longer focal length.

5.4 Conclusions

In this chapter, design, fabrication, and characterization of the liquid lens were discussed. Two methods for determining the focal length of the liquid lens were presented. The developed liquid lens responded to the applied electric potentials showing competitive electrowetting of the oil droplet. The shape change of the oil droplet, due to competitive electrowetting, enables the liquid lens to be a variable focal length lens. Fabrication technique involves only one mask layer and does not need a vertical electrode structure. The ring type electrodes are responsible for confining and focusing the liquid lens onto a plane.

The advantages of the liquid lens developed in this work are on-plane structure, simple fabrication, and a large focal length change. Due to these advantages, the developed microfluidic or optical systems could be integrated on microfluidic or optical systems.

CHAPTER 6. CONCLUSIONS

6.1 Summary

This thesis studied the feasibility and characteristics of a variable focal length liquid lens, using a submersed immiscible droplet in an aqueous solution. An electrowetting concept was employed to control the focal length of the liquid lens. Silicone oil was employed as a submersed droplet to work as a liquid lens. Planar electrodes were placed under a hydrophobic layer to generate electrowetting on the oil and water interface. The planar design, as one of the unique features of the work in this thesis, can possibly enhance the capability of the liquid lens to integrate with various microfluidic or optical systems.

Concepts and brief histories of surface energy, surface tension, electrowetting, and competitive electrowetting were discussed in Chapters 3 and 4. In order to validate electrowetting and competitive electrowetting, solid substrates with an electrode, covered by an insulator and a hydrophobic layer, were fabricated for the experiments. Cytop® formed a hydrophobic layer to act as an electrowetting substrate. Fabricated testing structures measured contact angle changes by electrowetting and competitive electrowetting. The measurement results were in agreement with those expected.

Based on the measurements from Chapters 3 and 4, a variable focal length liquid lens was designed, fabricated, and characterized in Chapter 5, using ring electrodes underneath a Cytop® layer as the hydrophobic surface and a Parylene layer as the conformal insulator. A submersed, silicone, oil droplet worked as the liquid lens. As the oil droplet changed its shape, it also changed the focal length with an applied electric potential. The focal length of the liquid lens with a diameter of 3 mm varied from 16.2 mm to 22.2 mm through electrowetting. By

combining competitive electrowetting technology, a more reliable liquid lens design could be created. Although the liquid lens devices would still be susceptible to integration, this model shows the feasibility of a future, integrated, liquid lens. This on-plane structure has an advantage of design flexibility in microsystems.

6.2 Future Research

On the liquid lens, the focal length was shown to be dependent on the electric voltage, but the related aberration and optical quality was not clearly provided in this work. As a result, there are many challenges motivated for future research.

The aluminum electrodes can degrade optical qualities of the liquid lens. Usually, most micro-optical devices use indium tin oxide (ITO) as the electrode material. Future work could apply the liquid lens with ITO electrodes to overcome optical quality problems. The introduction and submersion of silicone oil droplets is a cumbersome process, which makes it difficult to accurately control the volume of the oil droplet. An integrated liquid injection feature will improve the reliability of the liquid lens. To confine the oil droplet in the water, the study used pre-charged hydrophilic electrodes, a challenge of the developed liquid lens. Either a passive hydrophilic patch or no pre-charged hydrophilic patch would be desired. Recently, huge challenges for developing lab-on-a-chip systems are in high demand for study. The planar liquid lens, with its on-plane design, is an attractive aspect. Therefore, these works would continue to be applicable to integrate lab-on-a-chip systems.

REFERENCES

[1] J. C. Berg, *Wettability*, New York, Basel and Hong Kong: Marcel Dekker Inc., 1993.

[2] A. W. Adamson, *Physical Chemistry of Surfaces, 2nd ed.,* New York, London and Sydney: John Wiley & Sons Inc., 1967.

[3] S. Kuiper and B. H. W. Hendriks, "Variable-focus Liquid Lens for Miniature Cameras," *Applied Physics Letters,* vol. 85, pp. 1128-1130, August 2004.

[4] B. Berge and J. Peseux, "Variable Focal Lens Controlled by an External Voltage: An Application of Electrowetting," *The European Physical Journal E,* vol. 3, pp. 159-163, March, 2000.

[5] T. Krupenkin, S. Yang, and P. Mach, "Tunable Liquid Microlens," *Applied Physics Letters,* vol. 82, pp. 316-318, January 2003.

[6] E. Hecht, *Optics, 2nd ed.,* Massachusetts: Addison-Wesley Publishing Company., April 1988.

[7] R. Völkel, M. Eisner and K. J. Weible, "Miniaturized Imaging Systems," *Microelectronic Engineering*, vol. 67-68, pp. 463-472, September 2003.

[8] R. Irawan, C. M. Tay, S. C. Tjin and C. Y. Fu, "Compact Fluorescence Detection using In-fiber Microchannels-its Potential for Lab-on-a-chip Applications," *Lab on a chip,* vol. 6, pp. 1095-1098, June 2006.

[9] M. Yamauchi, M. Tokeshi, J. Yamaguchi, T. Fukuzawa, A. Hattori, A. Hibara, and T. Kitamori, "Miniaturized Thermal Lens and Fluorescence Detection System for Microchemical Chips," *Journal of Chromatography A,* vol. 1106, pp. 89-93, November 2005.

[10] N. R. Smith, D. C. Abeysinghe, J. W. Haus, and J. Heikenfeld, "Agile Wide-angle Beam Steering With Electrowetting Microprisms," *Optics Express,* vol. 14, pp. 6557-6563, July 2006.

[11] H. Okayama, "Design Criterion for Micro-machine Scanner Optical Switch Based on Beam Steering Angle Error Analysis," *Optical Review,* vol. 8, pp.294-300, April 2001.

[12] Y.-A. Peter, H. P. Herzig, and R. Dändliker, "Microoptical Fiber Switch for a Large Number of Interconnects: Optical Design Considerations and Experimental Realizations Using Microlens Arrays," *IEEE Journal on Selected Topics in Quantum Electronics,* vol. 8, pp. 46-57, February 2002.

[13] A. Tuantranont, V. M. Bright, J. Zhang, W. Zhang, J. A. Neff, and Y. C. Lee, "Optical Beam Steering Using MEMS-controllable Microlens Array," *Sensors and Actuators A,* vol. 91, pp. 363-372, June 2001.

[14] Z. D. Popovic, R. A. Sprague, and G. A. Neville Connell, "Technique for Monolithic Fabrication of Microlens Arrays," *Applied Optics,* vol. 27, pp. 1281-1284, April 1988.

[15] H. Ren, Y.-H. Lin, and S.-T. Wu, "Flat Polymeric Microlens Array," *Optics Commnuications,* vol. 261, pp. 296-299, May 2006.

[16] S. Haselbeck, H. Schreiber, J. Schwider, and N. Streibl, "Microlenses Fabricated by Melting a Photoresist on a Base Layer," *Optical Engineering,* vol. 32, pp. 1322-1324, June 1993.

[17] C.-Y. Chang, S.-Y. Yang, L.-S. Huang, and K.-H. Hsieh, "Fabrication of Polymer Microlens Arrays Using Capillary Forming with a Soft Mold of Micro-holes Array and UV-curable Polymer," *Optics Express,* vol. 14, pp. 6253-6258, June 2006.

[18] W. S. N. Trimmer, "Microrobots and Micromechanical Systems," *Sensors and Actuators A,* vol. 19, pp. 267-287, September 1989.

[19] G. F. Elliott and S. A. Hodson, "Cornea, and the Swelling of Polyelectrolyte Gels of Biological Interest," *Reports on Progress in Physics,* vol. 61, pp. 1325-1365, March 1998.

[20] M. Agarwal, R. A. Gunasekaran, P. Coane, and K. Varahramyan, "Polymer-based Variable Focal Length Microlens System," *Journal of Micromechanics and Microengineering,* vol. 14, pp. 1665-1673, August 2004.

[21] N. Chronis, G. L. Liu, K.-H. Jeong, and L. P. Lee, "Tunable Liquid-filled Microlens Array Integrated with Microfluidic Network," *Optics Express,* vol. 11, pp. 2370-2379, September 2003.

[22] W. Wang and J. Fang, "Variable Focusing Microlens Chip for Potential Sensing Applications," *IEEE Sensors Journal,* vol. 7, pp. 11-18, January 2007.

[23] L. G. Commander, S. E. Day, and D. R. Selviah, "Variable Focal Length Microlenses," *Optics Commnuications,* vol. 177, pp. 157-170, February 2000.

[24] J. C. Lötters, W. Olthuis, P. H. Veltink, and P. Bergveld, "The Mechanical Properties of the Rubber Elastic Polymer Polydimethylsiloxane for Sensor Applications," *Journal of Micromechanics and Microengineering,* vol. 7, pp. 145-147, April 1997.

[25] D.-Y. Zhang, V. Lien, Y. Berdichevsky, J. Choi, and Y.-H. Lo, "Fluidic Adaptive Lens with High Focal Length Tunability," *Applied Physics Letters,* vol. 82, pp. 3171-3172, May 2003.

[26] P. M. Moran, S. Dharmatilleke, A. H. Khaw, K. W. Tan, M. L. Chan, and I. Rodriguez, "Fluidic Lenses with Variable Focal Length," *Applied Physics Letters,* vol. 88, pp. 041120-1-041120-3, January 2006.

[27] R. A. Paxton, A. M. Al-Jumaily, A. J. Easteal, "An Experimental Investigation on the Development of Hydrogels for Optical Applications," *Polymer Testing,* vol. 22, pp. 371-374, January 2003.

[28] Y. Bar-Cohen, *Electroactive Polymer (EAP) Actuators as Artificial Muscles, 2nd ed.,* Washington: SPIE PRESS, 2004.

[29] P. G. De Gennes and J. Prost, *The Physics of Liquid Crystals, 2nd ed.,* Oxford: Clarendon Press, 1993.

[30] K. Kishikawa, M. C. Harris, and T. M. Swager, "Nematic Liquid Crystals with Bent-rod Shapes: Mesomorphic Thiophenes with Lateral Dipole Moments," *Chemistry of Materials,* vol. 11, pp. 867-871, March 1999.

[31] H. Knobloch, H. Orendi, M. Büchel, T. Seki, S. Ito, and W. Knoll, "Command Surface Controlled Liquid Crystalline Waveguide Structures as Optical Information Storage," *Journal of Applied Physics,* vol. 76, pp. 8212-8214, December 1994.

[32] S. Sato, "Liquid-crystal Lens-cells with Variable Focal Length," *Japanese Journal of Applied Physics,* vol. 18, pp. 1679-1684, September 1979.

[33] M. Ye, B. Wang, and S. Sato, "Double-layer Liquid Crystal Lens," *Japanese Journal of Applied Physics,* vol. 43, pp. L352-L354, February 2004.

[34] M. Ye, B. Wang, and S. Sato, "Driving of Liquid Crystal Lens without Disclination Occurring by Applying In-plane Electric Field," *Japanese Journal of Applied Physics,* vol. 42, pp. 5086-5089, August 2003.

[35] D. Psaltis, S. R. Quake, and C. Yang, "Developing Optofluidic Technology through the Fusion of Microfluidics and Optics," *Nature,* vol. 442, pp. 381-387, July 2006.

[36] F. Mugele and J. Baret, "Electrowetting: from Basics to Applications," *Journal of Physics: Condensed Matter,* vol. 17, pp. R705-R774, July 2005.

[37] C. Gabay, B. Berge, G. Dovillaire, and S. Bucourt, "Dynamic Study of a Varioptic Variable Focal Lens," *Proceedings of SPIE,* vol. 4767m pp. 159-165, July 2002.

[38] P. G. de Gennes, "Wetting: Statics and Dynamics," *Reviews of Modern Physics,* vol. 57, pp. 827-864, July 1985.

[39] R. J. Good, "Contact Angle, Wetting, and Adhesion: a Critical Review," *Journal of Adhesion Science Technology,* vol. 6, pp. 1269-1302, July 1992.

[40] N. A. Campbell, *Biology, 3rd ed.,* California: The Benjamin/Cummings Publishing Company, Inc., 1993.

[41] C. Quilliet, and B. Berge, "Electrowetting: a Recent Outbreak," *Current Opinion in Colloid and Interface Science,* vol. 6, pp. 34-39, June 2001.

[42] F. Mugele, A. Klingner, J. Buehrle, D. Steinhauser, and S. Herminghaus, "Electrowetting: a Convenient Way to Switchable Wettability Patterns," *Journal of Physics: Condensed Matter,* vol. 17, pp. S559-S576, February 2005.

[43] H. J. J. Verheijen and M. W. J. Prins, "Contact Angles and Wetting Velocity Measured Electrically," *Review of Scientific Instruments,* vol. 70, pp. 3668-3674, June 1999.

[44] J. Kim, W. Shen, L. Latorre, and C.-J. Kim, "A Micromechanical Switch with Electrostatically Driven Liquid-metal Droplet," *Sensors and Actuators A,* vol. 97-98, pp. 672-679, January 2002.

[45] S. K. Cho, H. Moon, and C.-J. Kim, "Creating, Transporting, Cutting, and Merging Liquid Droplets by Electrowetting-based Actuation for Digital Microfluidic Circuits," *Journal of Microelectromechanical Systems,* vol. 12, pp. 70-81, February 2003.

[46] J. Lee, H. Moon, J. Fowler, T. Schoellhammer, and C.-J. Kim, "Electrowetting and Electrowetting-on-dielectric for Microscale Liquid Handling," *Sensors and Actuators A,* vol. 95, pp. 259-268, September 2002.

[47] B. Janocha, H. Bauser, C. Oehr, H. Brunner, and W. Göpel, "Competitive Electrowetting of Polymer Surfaces by Water and Decane," *Langmuir,* vol. 16, pp. 3349-3354, February 2000.

VITA

      Jihwan Park was born and reared in Seoul, Korea, in October of 1974. He graduated from Korea Military Academy in 1997, and received his bachelor degree, having pursued a double major in computer science and military strategy. He has worked in the Korea military for ten years, where he served as a battery commander on the front line for four years. Mr. Park studied in the United States Army Field Artillery School, completing a captain's career course in 2001. Having completed the requirements for a master's degree at the Louisiana State University in engineering, he will join the Korea Military as an officer.